Why do ants differ in acclimatory ability? Biophysical mechanisms behind cuticular hydrocarbon acclimation across species

Lucas Baumgart[1,2,3], Marti Wittke[1], Svenja Morsbach[4], Bérengère Abou[3] & Florian Menzel[1*]

[1]Institute of Organismic and Molecular Evolution (iomE), Johannes Gutenberg-University Mainz, Hanns-Dieter-Hüsch-Weg 15, 55128 Mainz, Germany

[2]Institute of Biology II, RWTH Aachen University, Worringerweg 2, 52074 Aachen, Germany

[3]Matière et Systèmes Complexes (MSC), UMR CNRS 7057, Université de Paris, 75205 Paris Cedex 13, France

[4]Max Planck Institute for Polymer Research, Ackermannweg 10, 55128 Mainz, Germany

*Corresponding author: menzelf@uni-mainz.de

ORCID ID: LB: 0000-0003-1006-0659

FM: 0000-0002-9673-3668

Abstract

Maintaining water balance is vital for terrestrial organisms. Insects protect themselves against desiccation via cuticular hydrocarbons (CHCs). CHC layers are complex mixtures of solid and liquid hydrocarbons, with a surprisingly diverse composition across species. This variation may translate to differential phase behaviour, and hence varying waterproofing capacity. This is especially relevant when temperatures change, which requires acclimatory CHC changes to maintain waterproofing. Nevertheless, the physical consequences of CHC variation are still little understood. We studied acclimatory responses and their consequences for CHC composition, phase behaviour, and drought survival in three congeneric ant species. Colony fragments were kept under cool, warm, and fluctuating temperature regimes. *Lasius niger* and *platythorax*, both of which are rich in methyl-branched alkanes, showed largely predictable acclimatory changes of the CHC profile. In both species,

warm acclimation increased drought resistance. Warm acclimation increased the proportion of solid compounds in *L. niger* but not in *L. platythorax*. In both species, the CHC layer formed a liquid matrix of constantly low viscosity, which contained highly viscous and solid parts. This phase heterogeneity may be adaptive, increasing robustness to temperature fluctuations. In *L. brunneus*, which is rich in unsaturated hydrocarbons, acclimatory CHC changes were less predictable, and warm acclimation did not enhance drought survival. The CHC layer was more homogenous, but matrix viscosity changed with acclimation. We showed that ant species use different physical mechanisms to enhance waterproofing during acclimation. Hence, the ability to acclimate, and thus climatic niche breadth, may strongly depend on species-specific CHC profile.

Keywords: climate adaptation, cuticular hydrocarbons, ecological niche breadth, phase behaviour, microrheology, drought tolerance

Introduction

All terrestrial organisms need to maintain their water balance to survive (Chown, Sørensen & Terblanche 2011; Kellermann *et al.* 2012). Due to their high surface-to-volume ratio (Gibbs 1998; Blomquist & Bagnères 2010), insects are particularly prone to desiccation. They mostly lose water via transpiration through the cuticle, which accounts for 80% of the total water loss (Gibbs & Rajpurohit 2010). In times of climate change with increased probability of heat and drought waves, desiccation risk will increase for many insect species, and they will need to cope with higher water stress. Insects can reduce water loss via behavioural changes, e.g., movement to a more humid place (Spicer *et al.* 2017). However, the main barrier against water loss is their cuticular hydrocarbon layer. Cuticular hydrocarbons (CHCs) cover the body surface of virtually all insects. Beside their waterproofing function, they carry vital communication signals (Leonhardt *et al.* 2016), and serve other functions such as lubricating the cuticle (Cooper *et al.* 2008) and the enhancement of foot adhesion (Drechsler & Federle 2006).

Cuticular hydrocarbon profiles show an astonishing diversity across species (Kather & Martin 2015; Sprenger & Menzel 2020). Even sister species can have radically different profiles (Pokorny *et al.* 2014; Hartke *et al.* 2019). Despite intraspecific variation, the profiles are specific enough so that species can clearly be identified based on their profile (Kather & Martin 2012). Some of this diversity might be due to the role of CHCs as communication signals and/or mating signals, which can require complex profiles and/or lead to sexual selection (Ferveur & Cobb 2010; Steiger & Stökl 2014; Leonhardt *et al.* 2016). However, the composition of a CHC layer also determines its waterproofing ability. Hence, species from wet habitats often possess different profiles than those from drier ones (Van Wilgenburg, Symonds & Elgar 2011; Menzel, Blaimer & Schmitt 2017). Moreover, insects have to adjust their CHC composition to current conditions, and this affects their subsequent drought

survival (Toolson & Hadley 1979; Menzel, Zumbusch & Feldmeyer 2018; Sprenger *et al.* 2018). So how does waterproofing work on a physical level, and how does CHC composition affect that?

Generally, the CHC layer reduces water loss by forming a passive barrier against outward diffusion of water. The effectiveness of this barrier is given by its proportion of solid components (which block diffusion more effectively), and by its viscosity: according to the Stokes-Einstein relation, the diffusion coefficient of molecules is inversely proportional to viscosity (Einstein 1905); hence water diffusion should decrease with increasing viscosity of the CHC layer. CHC layers are complex mixtures of sometimes more than 100 different hydrocarbons (Blomquist & Bagnéres 2010). They include *n*-alkanes, methyl-branched components and unsaturated hydrocarbons with chain lengths ranging from 21 to 50 carbons (Blomquist & Bagnères 2010). Due to van der Waals forces, hydrocarbons tend to aggregate. *n*-alkanes pack most tightly, being solid at ambient temperatures (Maroncelli *et al.* 1982) and melting only at temperatures > 40 °C (Lide 2008). In contrast, methyl groups or double bonds hinder tight packing and thus strongly reduce melting temperatures (Gibbs & Pomonis 1995; Gibbs 1998; Gibbs 2002). As a consequence, alkenes, and at least some methyl-branched alkanes are liquid at ambient temperature. For the same chain length, the melting temperature decreases in the order *n*-alkanes, mono-methyl alkanes, di-methyl alkanes, alkenes and alkadienes (Gibbs 1998). In addition, the position of the methyl branch affects melting, with more terminally branched alkanes having higher melting temperatures (Gibbs & Pomonis 1995). Melting points also increase with chain length (Gibbs & Pomonis 1995).

Therefore, the CHC layer is not uniform, but rather a mixture of solid and liquid compounds. The phase behaviour of the CHC layer, and thus its ability to prevent evaporation, continuously changes as temperatures rise or fall – with higher temperatures, some solid CHCs may melt, and some liquid CHCs may become less viscous. As a consequence, insects adjust the CHC composition to current temperature or humidity conditions (Hadley 1977). With increasing temperatures, *n*-alkanes increase while methyl-branched alkanes decrease (Gibbs & Mousseau 1994; Buellesbach *et al.* 2018; Menzel, Zumbusch & Feldmeyer 2018; Michelutti *et al.* 2018; Sprenger *et al.* 2018). However, it is still unknown how the chemical changes translate to the physical properties that determine the waterproofing ability – melting range (and hence, the proportion of solid CHCs) and viscosity. For insects, an important challenge here are fluctuating temperatures, which often pose requirements entirely different from constant environments (Colinet *et al.* 2015). Here, it is crucial that a CHC layer maintains its waterproofing ability even when temperatures suddenly drop or rise. In general, however, the complexity of CHC profiles makes it difficult to predict their physical behaviour. Hence, we need to understand the physical mechanisms of waterproofing, as well as the effects of acclimatory changes, to fully appreciate how CHC composition determines the climatic niche of an insect.

In this work, we investigated acclimation and its biological, chemical, and physical consequences in three species of the ant genus *Lasius*. *Lasius niger*, *L. platythorax* and *L. brunneus* all have different CHC profiles, and, while sympatric in Central Europe, occur in different habitats (Seifert 2008). Our

aim was to investigate species-specific acclimation responses of their CHC profile to different temperatures and their effects on drought survival at different temperatures. Using a microrheology technique that has been adapted for the study of insects (fluid quantities of the order of 100 pL) (Abou *et al.* 2010), as well as differential scanning calorimetry (DSC), we aimed to find links between the CHC profile, its physical properties, and the ants' ability to enhance drought resistance via acclimation. Our research questions were:

- how do acclimatory CHC changes differ between ant species?
- how do acclimatory changes translate to the phase behaviour of the CHC layer, i.e. how is waterproofing achieved on a physical level?
- do acclimatory strategies differ between species, and how do they affect drought survival?

Material and Methods

Study organisms and setup of experimental colonies

We investigated three ant species: *Lasius niger, L. platythorax* and *L. brunneus*, all of which occur in central Europe. From each species, we collected twelve colonies in the surroundings of Mainz, Germany (*L. niger*: on meadows near the University of Mainz; *L. platythorax*: from the forest floor of the Ober-Olmer forest; *L. brunneus* at tree trunks in the Gonsenheimer forest). Each colony of *L. niger* and *L. platythorax* was divided into two groups for a separate study (Wittke et al. 2022). Each of the two groups then was further split up into three fragments. Fragments of group 1 ('small boxes') were kept in small plastic boxes (95×95×60 mm, Westmark GmbH, Lennestadt-Elspe, Germany) with plastered ground and a cavity (ca. 50×30×3 mm) covered with glass plates and red foil and walls coated with Fluon® (Whitford GmbH, Diez, Germany). Each box consisted of 20 foragers (collected outside the nest), 20 nurses (collected inside the nest, if possible, directly from the brood), at least five brood items, mostly larvae and in some cases pupae and no queens. Group 2 fragments ('large boxes') were kept in 3 larger plastic boxes (235×175×90 mm) with plastered ground and walls coated with Fluon®; they were kept in their original nesting material (i.e., soil for *L. niger* and soil, pieces of wood, and moss, for *L. platythorax*). Each group 2 box consisted at least 60 foragers (collected outside the nest), 60 nurses (collected inside the nest, if possible, directly from the brood) and at least 20 brood items, mostly larvae and in some cases pupae. Except for one box (*L. platythorax*, fluctuating treatment), all group 2 boxes were queenless as well. For *Lasius brunneus*, we only had group 1 boxes, because this is an arboreal species, such that we could not collect entire colonies without destroying the nest tree. Here, we used worker groups, which were divided into three fragments per colony as above. Each box consisted of at least 20 foragers (collected outside the nest) and no brood items, because these could not be collected due to their arboreal nesting. All boxes were covered with lids and sealed with Parafilm™ (Bemis Flexible Packaging, neetah, WI, USA) to ensure constant humidity. Honey, dead crickets, and water in Eppendorf cups (Eppendorf AG, Hamburg, Germany)

with a cotton plug were provided twice a week *ad libitum*. See Fig. 1 for a visual guide for the used methodology.

Acclimation treatments

We set up three temperature treatments: constant temperature at 20 °C, 28 °C and a fluctuating treatment. The fluctuating treatment had 20 °C at night (8 hours) and 28 °C during the day (8 hours), with 4 h ramps between the two temperatures. All treatments had a 12 h:12 h light:dark cycle. Relative humidity inside these stock colonies was kept at nearly 100% by placing water on the plaster until it was saturated. All climate treatments were maintained in climate cabinets (Rubarth Apparate GmbH, Frankfurt am Main, Germany). Climatic conditions were surveyed using data loggers (testo 174H, Testo SE & Co. KGaA, Titisee-Neustadt, Germany). From each source colony, we placed one small and (for *L. niger* and *L. platythorax*) one large fragment in each of the three climate treatments and let the ants acclimate for three weeks.

Chemical analysis

After three weeks of acclimation, we analysed the chemical profile of the ants (total n = 360). We used two outside workers (foragers), from each large box of *L. niger* and *L. platythorax* and from the small boxes of *L. brunneus* ($N_{L.\ niger}$ = 66; $N_{L.\ brunneus}$ = 54; $N_{L.\ platythorax}$ = 57), as well as two nurses of each small box of *L. niger* and *L. platythorax* ($N_{L.\ niger}$ = 72; $N_{L.\ platythorax}$ = 67). Each worker was placed individually into a 1.5 mL glass vial (Chromatographie Zubehör Trott, Kriftel, Germany) and frozen at -20 °C until extraction. CHCs were extracted by immersing the ant for 10 minutes in *n*-hexane; we added 100 ng *n*-octadecane (solved in 10 µL *n*-heptane) as internal standard for quantification of the absolute CHC amount. The samples were concentrated under a gentle nitrogen flow down to approx. 20 µL.

For each sample, 2 µL were injected into the GC (7890A, Agilent Technologies, Santa Clara, CA, USA) at 250 °C in splitless mode. The carrier gas used was helium at a flow rate of 1.2 mL min^{-1} and the stationary phase was a Zebron Inferno DB5-MS capillary column (length 30 m, diameter 0.25 mm, 0.25 µm coating, Phenomenex Ltd, Aschaffenburg, Germany). About 50% of the samples were injected after a 10 cm column shortening. The temperature program started at 60 °C. After 2 min, the oven heated at a rate of 60 °C min^{-1} up to 200 °C and afterwards at a constant rate of 4 °C min^{-1} up to 320 °C, where it was held for constant 10 minutes. In the MS (5975C, Agilent Technologies) the hydrocarbons were fragmented with an ionization voltage of 70 eV. The detector scanned for molecular fragments in a range of 40-550 m/z.

We evaluated the data using the software MSD ChemStation (E.02.02. 1431, Agilent Technologies). The integration of the peaks of *L. niger* and *L. platythorax* were performed by two persons (LB and MW), whereas all peaks of *L. brunneus* were integrated by LB only. We identified the hydrocarbons based on a retention index based on a standard series of *n*-alkanes (Carlson et al. 1998) and diagnostic ions. Non-hydrocarbon substances, hydrocarbons with a maximum (across all samples per species) below 0.5% and hydrocarbons that occurred in less than 20% of the samples of either species or treatment were excluded.

To test for effects of acclimation treatments, we firstly analysed univariate CHC traits, and secondly the entire CHC composition. The CHC traits were the proportions of CHC classes (*n*-alkanes, mono-methyl, di-methyl and tri-methyl alkanes, alkenes, methyl alkenes and alkadienes), average chain length of *n*-alkanes, and the absolute CHC quantity. For each trait and ant species, we constructed a separate linear mixed-effects (LMM) model (command *lmer*, package *lme4 (Bates et al. 2011)*) with *acclimation regime* (20°C, 28°C or fluctuating) and *fragment type* (small/large) as fixed factors (interactions allowed), and *colony* and (if applicable) *observer* as random effects. The dependent variables were transformed if necessary to obtain normally distributed model residuals (Tab. 1).

For the entire CHC composition, we used the proportions of all CHC classes (*n*-alkanes, monomethyl, dimethyl, trimethyl alkanes, alkenes, alkadienes, methyl alkenes, and unknown CHCs) which added up to 1. This dataset was analysed using a PERMANOVA with the fixed factors *constant/fluctuating* and *temperature* (20 °C vs 28 °C; nested within *constant/fluctuating*) and *colony* (R command *adonis*, package *vegan (Oksanen et al. 2013)*). Interactions between the factors were allowed. Fragment type (small vs. large) was used as random factor (strata) except for *L. brunneus*, where there were no large fragments. This setup was used in order to test whether the fluctuating profile differed systematically from the two constant regimes, or whether it varied on the same axis as the two constant regimes. The PERMANOVA tests were done for each species separately. All statistical analyses were carried out using R v. 4.1.0 (www.r-project.org).

Differential Scanning Calorimetry

Melting ranges were determined using differential scanning calorimetry (DSC). We produced separate extracts for each colony in order to obtain replicates. To obtain analysable DSC data, a high number of workers is required to extract enough sample mass. For this reason, samples for DSC could only be obtained for *L. niger* and *L. platythorax* (sample sizes *L. niger*: $N = 18$ colonies; *L. platythorax*: $N = 26$ colonies) whereas we did not have enough *L. brunneus* workers required for DSC. Hexane extracts were directly transferred into DSC sample aluminum pans (100 µL volume, Mettler-Toledo GmbH, Gießen, Germany) and the solvent evaporated slowly under ambient conditions. DSC pans were covered with aluminum lids.

DSC measurements were performed on a DSC 823 instrument (Mettler-Toledo GmbH, Gießen, Germany). Heating-cooling-heating cycles were recorded with a heating/cooling rate of 10 K min^{-1} between -100 and +100 °C. The measurements were performed under nitrogen atmosphere with a flow of 30 mL min^{-1}. For determination of melting ranges, the second heating cycle was evaluated to avoid effects due to sample history. Heating curves were baseline-corrected and normalized to the sample mass. For further data analysis, all melting curves for the respective acclimatization treatment were then averaged and subsequently integrated in 10 K intervals between -60 °C and +60 °C to yield the proportionate amount of melting heat for each interval (and in addition, the interval between 20 and 28 °C). No significant melting was detected between -100 °C and -60 °C and between +60 °C and +100 °C. Each interval was then analysed using linear models with the fixed factors species, acclimation, and their interaction.

Microrheology

The phase behaviour and viscosity of CHCs from the three *Lasius* species were studied using a newly developed fluid collection procedure for insect secretion, followed by a microrheology technique adapted to small amounts of fluid of the order of 100 pL (Abou et al. 2010). For each *Lasius* species, we measured viscosity of one forager CHC extract (without internal standard) per colony and per acclimation treatment (n = 6 colonies for *L. platythorax* and *L. brunneus*, n = 5 colonies for *L. niger*; total N = 51 samples).

Each CHC extract was evaporated, resolved in 40 µL *n*-pentane for 15 min, and transferred onto a microscopic slide. After the pentane was evaporated, the CHCs were sucked up by a microsyringe with a tip of a few micrometers mounted on a three-axis piezo micromanipulator (Burleigh, Thorlabs SAS, Maisons-Laffitte, France), itself coupled to an inverted microscope (Leica DM IRB, Leica Microsystems GmbH, Germany), using capillary effects. For highly viscous CHCs, we applied negative pressure to the microsyringe using the microinjector (CellTram Air, Eppendorf AG, Hamburg, Germany) for collection. Dry powder of melamine beads (diameter: 0.740 ±0.005 µm; Acil, France) was deposited on a cover slip, and the collected CHCs were ejected onto the beads by applying positive pressure (Abou et al. 2010).

The motion of the tracer beads immersed in the CHC drop was recorded with a fast sCMOS camera (OrcaFlash 4.0 v2+, Hamamatsu Photonics France S.A.R.L., France) attached to the microscope with an oil immersion objective (100X). The camera sampled at 100 Hz at five different temperatures (30, 28, 24, 20 and 18 °C) for 20 s each. Temperatures were adjusted by an objective heater (Bioptechs Inc., Butler, PA, USA), with an accuracy of ± 0.1 °C. Using self-written image analysis software under ImageJ (Rasband, W.S., ImageJ, U. S. National Institutes of Health, Bethesda, Maryland, USA, https://imagej.nih.gov/ij/, 1997-2018.), the $x_i(t)$ and $y_i(t)$ positions of the beads were tracked and the

mean-squared displacement (MSD) was calculated for each individual bead or averaged over several beads according to:

$$< \Delta r^2(\mathrm{t}) >=< \left(x_i(t'+t) - x_i(\mathrm{t}')\right)^2 + (y_i(\mathrm{t}'+t) - y_i(\mathrm{t}'))^2 >_{\mathrm{i,t}'}$$

For a purely viscous fluid, the MSD is expressed as $< \Delta r^2(t) >= 4D\mathrm{t}$ giving access to the diffusion coefficient D and then to the viscosity η from the Stokes-Einstein relation $\eta = kT/6\pi RD$, where R is the bead radius, k is the Boltzmann constant and T is the temperature in Kelvin (Einstein 1905). Most samples contained a multiphasic liquid, with highly different viscosities per phase. However, the least viscous phase was by far the most abundant, as measured by the number of beads with similar viscosities. This heterogeneity of viscosities (liquid phase only) declined at higher temperatures, such that the collected samples had a homogeneous viscosity at temperatures of 28°C or higher. Due to the heterogeneity of the collected CHC, we conducted two different analyses: firstly, we measured the viscosity of each single bead in all samples at 24°C for comparison. Secondly, we focused on the least viscous phase in all samples, and analysed its viscosity at all measurement temperatures spanning 18°C to 32°C.

The single-bead viscosity data were highly non-normally distributed. Therefore, we used geometric means to characterize the distribution of the single-bead viscosity data. Geometric means of all beads per sample were calculated as the exponential of the arithmetic mean of log-transformed viscosity data. In analogy, geometric standard deviation was calculated as the exponential of the standard deviation of log-transformed data. As a measure of heterogeneity per sample, we then calculated the coefficient of variation (CV) as the variation in viscosity. The geometric means and the geometric CVs were then compared using linear mixed-effects models (LMM), with acclimation treatment and species as fixed factors and colony ID as random factor.

For the least-viscous phase per sample, the relation between viscosity (as dependent variable) and measurement temperature was first assessed using non-linear least square models (NLS). Normally distributed model residuals were only obtained after log-transformation of viscosity data. Model fits were equally good whether temperature was denoted as 1/T (in K^{-1}) or T (in °C). Concerning AIC, linear dependence on measurement temperature was as good as exponential or square-root relations (all $\Delta AIC \leq 0.067$), but significantly better than a quadratic term. Hence, we described the data using the Arrhenius law, with a linear relation between log (viscosity) and the inverse temperature (1/T in K^{-1}) (De Guzmán 1913; Eyring 1935). In a next step, we created linear mixed-effects (LMM) models with species, acclimation treatment and measurement temperature as explanatory variables, with all interactions allowed and colony ID as random effect. Non-significant interactions were removed

stepwise by removing the least significant interaction until AIC was minimal. All models were analysed using *Anova* (package *car;* (Fox et al. 2012).

Drought survival

We measured drought survival at two different temperatures (20 °C and 28 °C, henceforth termed 'test temperatures') for each species and acclimation treatment. To this end, we used foragers from each large box (small box for *L. brunneus*). Two foragers were used per species, colony, acclimation treatment and test temperature, resulting in 432 replicates. Foragers were placed individually into a polystyrene vial (Ø 28 mm, height 64 mm, volume 30 ml, K-KTK e.K., Retzstadt, Germany). It was plugged with a piece of foam (12.05 ± 0.94 mm) to approximately one third of its height, filled with silica gel (2-5 mm, i.e., 7.98 ± 0.32 g, Sigma-Aldrich Laborchemikalien GmbH, Seelze, Germany) and sealed airtight with Parafilm™. Then the vials were placed into climate cabinets at 20 °C or 28 °C.

We checked survival first after 6 h for the 20 °C experiment series (after 4 h for *L. brunneus*), after 4 h for the 28 °C experiment series and afterwards once every hour until the 24th hour of the experiment. The death of an ant was defined here as the lack of any movement even after shaking the vial. All observations were conducted blindly.

As a control group we put two foragers of three colonies from each of the large boxes of *L. niger* and *L. platythorax* ($N_{L.\ niger} = 45$; $N_{L.\ platythorax} = 48$) with a piece of a wet paper towel individually into a polystyrene vial, plugged it with a piece of foam and sealed it with Parafilm™ to exclude death caused by isolation. In the control group, where we tested if the ants die from isolation rather than from drought stress only three ants out of 90 died within the 24 hours of the experiment.

The data was analysed with a Cox mixed-effects model (command *coxme*, R package *coxme*; Thereneau 2020) with species, acclimation temperature and experiment temperature as explanatory variables and colony ID and test day as random effects. The results for this model were too complex, which is why we created two different, more specific models. First, we created a test temperature-specific model with a subset of the data, which only contains test temperature 20 °C or 28 °C, with acclimation temperature and species as explanatory and colony ID and test day as random effects. Afterwards we checked effects species-wise for each test temperature. Second, we created a treatment-specific model with a subset of the data, which only contains the corresponding acclimation temperatures (20 °C, 28 °C and fluctuating) with test temperature and species as explanatory and colony ID and test day as random effects. Afterwards we checked effects test temperature-wise for each species. Only few ants had died before the first observation, i.e. in the first 6 h ($N_{L.\ niger} = 6$, $N_{L.\ platythorax} = 1$; $N_{L.\ brunneus} = 23$) or 4 h, respectively ($N_{L.\ niger} = 12$, $N_{L.\ platythorax} = 1$; $N_{L.\ brunneus} = 34$). Since their time of death was uncertain, we conducted two parallel analysis, treating them as if they had died a) in the first hour of the experiment or b) directly before the first observation. The two analyses yielded comparable results, and we focus on analysis a) in the results, but report analyses of b) in the

supplement. We tested variables with type-II ANOVA (command *Anova*, package *car*, Fox and Weisberg 2019). Pairwise comparisons were done using a Tukey post-hoc comparison (command *glht*, package *multcomp*; Hothorn et al. 2008).

Results

Chemical analysis: Overall CHC composition

All three species had very different CHC profiles (Fig. 2, Datasets S1-S3). *Lasius niger* and *L. platythorax* both were dominated by mono-, di- and tri-methyl alkanes. In *L. platythorax*, all monomethyl alkanes were internally branched. In *L. niger*, 6.2 ± 0.19% (mean and SE) out of 24.9 ± 0.30% were terminally branched (methyl branch positions 2 to 5). For *L. brunneus*, terminally branched monomethyl alkanes represented 3.72 ± 0.21% out of 10.3 ± 0.27% monomethyl alkanes. However, compared to *L. niger*, the profile of *L. platythorax* had higher chain lengths, more trimethyl alkanes, and fewer monomethyl alkanes. The profile of the third species, *L. brunneus*, differed strongly from the others. It was dominated by alkenes, methyl alkenes and alkadienes but had only few di- or trimethyl alkanes.

Chemical analysis: Acclimatory changes of CHC classes, chain lengths, and absolute quantity

All three species showed strong, and often parallel, responses to the acclimation regimes. Several CHC classes were lowest in the 20 °C treatment, highest at 28 °C and intermediate in the fluctuating treatment (Fig. 3), which would be expected for CHCs that are comparatively viscous or solid, and thus effective for waterproofing. This was true for *n*-alkanes and monomethyl alkanes in both *L. niger* and *L. platythorax*, and for alkenes in *L. brunneus* (Tab. 1). Other substances were most abundant at 20 °C, least abundant at 28 °C and intermediate in the fluctuating treatment, which would be expected for the less viscous CHCs. Indeed, this was true for dimethyl alkanes in *L. niger* and trimethyl alkanes in *L. platythorax*, and, although not all three treatments differed significantly from each other, for alkenes in *L. niger* and methylbranched alkenes in *L. brunneus* (Tab. 1). Abundances did not differ among treatments for trimethyl alkanes in *L. niger* and dimethyl alkanes in *L. platythorax* and *L. brunneus*. These CHC classes had abundances of < 7 %, with the notable exception of dimethyl alkanes in *L. platythorax*, which made up around 50 % of the profile. In three cases, fragment type affected CHC class abundance: *n*-alkanes (more in small fragments) in *L. platythorax*, and trimethyl alkanes in *L. niger* and *L. platythorax* (less in small fragments in both species; Tab. S1). Interactions between acclimation treatment and fragment type were never significant.

Only in *L. brunneus*, we found further acclimation effects that deviated from those described above (Tab. 1). In this species, *n*-alkanes were lowest in the fluctuating treatment but similarly high in the 20 °C and 28 °C regimes. The opposite was found for alkadienes, which were highest for the fluctuating regime, and did not differ between 20 °C and 28 °C regimes. Proportions of monomethyl alkanes in *L. brunneus* were highest in the 20 °C treatment but at a similarly lower level for the 28 °C and the fluctuating treatment. Furthermore, average chain length of *n*-alkanes in *L. brunneus* was much higher in the 28 °C and the fluctuating treatment compared to the 20 °C treatment ($\chi^2_2 = 54.45$, $p < 0.001$) (Fig. S1). In contrast, it did not differ among acclimation treatments in *L. niger* nor *L. platythorax* (both $\chi^2_2 < 1.3$, $p > 0.5$). Finally, in *L. brunneus*, all three acclimation treatments led to different absolute CHC quantities, with highest quantities at fluctuating conditions, intermediate at 28°C and lowest at 20°C ($\chi^2_2 = 22.81$, $p < 0.001$) (Fig. S1). In contrast, absolute CHC quantities were at most slightly affected by acclimation in *L. niger* and *L. platythorax*. In *L. niger*, quantities were slightly higher for 20°C-acclimated ants (albeit not in pairwise comparisons; $\chi^2_2 = 7.58$, $p = 0.02$), while there was no effect in *L. platythorax* ($\chi^2_2 = 1.92$, $p = 0.38$).

The deviant patterns of *L. brunneus* was also reflected in the overall CHC composition. Here, acclimation treatments affected the overall CHC composition in all three species. But only in *L. brunneus*, the fluctuating conditions systematically differed from constant ones (PERMANOVA: pseudo-$F_1 = 23.3$, $p = 0.001$, Tab. S2). This factor was not significant for *Lasius niger* and *L. platythorax*, indicating that here, the fluctuating treatment did not differ systematically from the constant ones, but rather resulted in CHC changes intermediate between the constant 20 °C and the constant 28 °C regime (pseudo-$F_1 = 0.80$, $p = 0.48$; pseudo-$F_1 = 1.3$, $p = 0.28$ for *L. niger* and *L. platythorax*). The two constant regimes (20 °C and 28 °C) differed from each other in all three ant species. See Tab. S2 for further details.

Overall, we found that in *L. niger* and *L. platythorax*, warm acclimation led to higher abundances of rather solid or viscous CHC classes, and lower abundances of less viscous CHC classes. The fluctuating treatment was in between the constant cool and the constant warm treatment. Hence, acclimatory changes in these two species were quite predictable overall. In *L. brunneus* in contrast, acclimatory changes were not in line with expectations, with several counter-intuitive changes. Most notably, the fluctuating treatment resulted in CHC changes that systematically differed from the two constant ones rather than being intermediate.

Biophysical analyses: Melting behaviour

In both ant species, CHC started to melt around -40 °C, and the last CHCs liquefied at 45-50 °C (Fig. 4). The largest melting peaks were observed between -25 °C and -5 °C, where 52.1 ± 3.0% (*L. niger*) and 57.5 ± 2.4% (*L. platythorax*) of all CHCs became liquid. Overall, melting ranges of *L. niger* and *L. platythorax* were surprisingly similar (Fig. 4). Especially the 20 °C-acclimated individuals of both

species were hardly different, whereas differences were more pronounced for ants from the 28 °C regimes. Interestingly, less than 7% of the CHCs melted between 20 °C and 28 °C, i.e. between the two acclimation temperatures. Acclimation did not affect this proportion (LM: $F_2 = 0.77$, $p = 0.47$). In this interval, slightly more CHCs melted in *L. niger* than in *L. platythorax* (LM: $F_1 = 4.80$, $p = 0.035$; species x acclimation: $F_2 = 0.14$, $p = 0.87$). Generally, around 90% or more of CHCs melted below 28°C. This proportion was only lower for warm-acclimated *L. niger*. In this species, ants from the 28 °C treatment had less CHCs melting below 28°C compared to the other two treatments (both $t > 2.9$, $p < 0.006$), whereas acclimation treatments did not differ in *L. platythorax* (LM: species: $F_1 = 5.7$, $p = 0.022$; acclimation: $F_2 = 2.1$; $p = 0.14$; interaction: $F_2 = 4.6$, $p = 0.017$) (Fig. 5).

To further analyse melting ranges, we divided them into 10 K intervals. Here, strong acclimatory effects were found for the 30-40 °C interval, where the proportion of melting CHCs was significantly higher for warm-acclimated ants, but only in *L. niger* (acclimation: $F_2 = 4.8$; $p = 0.014$; species: $F_1 = 11.2$, $p = 0.0018$; interaction: $F_2 = 5.3$; $p = 0.0094$) (Fig. 5). A similar, but weaker pattern was found for the 40-50 °C interval (acclimation: $F_2 = 2.2$; $p = 0.13$; species: $F_1 = 1.99$, $p = 0.17$; interaction: $F_2 = 3.2$; $p = 0.050$). In turn, slightly less CHCs melted in the -10 °C to 0 °C interval in warm-acclimated *L. niger* compared to the other climate regimes or to *L. platythorax* (acclimation: $F_2 = 2.6$; $p = 0.091$; species: $F_1 = 3.4$, $p = 0.075$; interaction: $F_2 = 0.78$; $p = 0.46$). Furthermore, warm-acclimated ants of both species had significantly fewer CHCs melting between 10 °C to 20 °C (acclimation: $F_2 = 7.3$; $p = 0.0020$; species: $F_1 = 1.3$, $p = 0.25$; interaction: $F_2 = 1.1$; $p = 0.35$). No other effects were found for any 10 K interval.

Overall, the melting profiles of *L. niger* and *L. platythorax* were remarkably similar (*L. brunneus* could not be analysed due to the high number of workers necessary for DSC). Interestingly, only few CHCs melted between 20 °C and 28 °C, and this amount was independent of acclimation treatment. Thus, irrespective of acclimation treatment, the proportion of solid CHCs at 20 °C was not much higher than at 28 °C. Acclimation effects were most notable in *L. niger*, where warm-acclimated ants had more CHCs melting between 30 and 50 °C, and fewer CHCs melting at temperatures below 20 °C. In *L. platythorax* in contrast, acclimation affected CHC melting much less, and especially above 30 °C no effect of acclimation was detectable.

Biophysical analyses: Phase behaviour

All CHC extracts were highly heterogeneous, with solid and liquid phases co-occurring even at 32 °C. However, even within the liquid phase, the samples developed a more heterogeneous phase behaviour with decreasing temperature, including signs of gelification (albeit less so in *L. brunneus*). This was reversible, i.e. all gelified parts liquefied when temperature was increased again. Heterogeneity was evidenced by closely spaced beads of different viscosities in the liquid phase of the same sample (Fig. S2). Across all species, the lowest viscosity level was most abundant, representing 77 % of the beads

(0.35 ± 0.06 mPa*s, n = 246 out of 319 beads) (Fig. 6). Therefore, viscosity was analysed firstly for all viscosity levels (but only at measurement temperature 24 °C), and secondly only for the most abundant, least viscous level (but all measurement temperatures). When including all beads, the (geometric) mean viscosity neither differed between species nor acclimation treatments (LMM, log-transformed data: both $\chi^2_2 \leq 2.7$, $p > 0.25$; interaction: $\chi^2_4 = 6.5$, $p = 0.16$) (Fig. 7A). However, the heterogeneity in viscosity (quantified as coefficient of variation, CV) differed between species: it was significantly lower in *L. brunneus* (LMM, square-root transformed data: $\chi^2_2 = 10.3$, $p = 0.0058$), indicating that CHC layers of *L. brunneus* are more homogenous. Heterogeneity also differed among acclimation treatments, being higher for the fluctuating treatment ($\chi^2_2 = 8.1$, $p = 0.017$). The interaction species:acclimation was not significant ($\chi^2_4 = 4.3$, $p = 0.37$) (Fig. 7B). Our second analysis considered only the least viscous phase (77 % of all beads). Here, we analysed the effect of measurement temperature, species and acclimation treatment in a parametric Arrhenius model. As expected, measurement temperature had the highest impact on viscosity (LMM: $\chi^2 = 103.5$, $p < 0.0001$). This effect was independent of acclimation and species, i.e. none of the samples was more or less sensitive to measurement temperature (no significant interactions with measurement temperature). Interestingly, acclimation only affected viscosity of this least viscous phase in *L. brunneus* (acclimation: $\chi^2 = 34.03$, $p < 0.001$; species: $\chi^2 = 16.28$, $p < 0.001$; interaction: $\chi^2 = 65.39$, $p < 0.001$). In this species, viscosity differed between all three acclimation treatments, being highest for the 20 °C treatment, intermediate for 28 °C, and lowest for the fluctuating treatment (Fig. 7C). For *L. niger* and *L. platythorax*, acclimation did not change viscosity, and their values were similar to the fluctuating treatment of *L. brunneus*.

Overall, the liquid phase of the CHCs was very heterogeneous, with patches of highly variable viscosity. While the average viscosity did not differ between species nor between acclimation treatments, CHCs of *L. niger* and *L. platythorax* were more heterogeneous compared to the more homogenous *L. brunneus*. Heterogeneity was also increased in fluctuating-acclimated ants. We then focused on the least viscous phase, which made up 77 % of all beads. This phase behaved as predicted by Arrhenius' law in terms of the relationship between viscosity and temperature. Interestingly, acclimation effects were only detected in *L. brunneus*, where viscosity was highest for 20 °C-acclimated ants, and lowest for fluctuating-acclimated ants. In the other two species, viscosity of the least viscous phase did not differ among acclimation treatments.

Drought Survival

Drought survival differed strongly among test temperatures, species, and acclimation treatments. The highest impact was test temperature – workers dried out faster at 28 °C (comprehensive Cox LME model, $\chi^2 = 138.24$, $p < 0.001$) (Fig. 8). In general, *L. platythorax* survived longer than the other two

species, but these differences were not always significant. Due to complex statistical interactions, we constructed separate models for the two test temperatures.

Under cooler conditions, acclimation and species identity affected survival much less. At 20 °C test temperature, *L. platythorax* always survived longer than the other two species (species $\chi^2_2 = 42.55$, $p < 0.0001$). This difference was highest for 28 °C-acclimated ants; in the fluctuating treatment it did not significantly differ from *L. niger* (acclimation: $\chi^2_2 = 4.88$, $p = 0.087$; species x acclimation: $\chi^2_4 = 11.5$, $p = 0.021$; Tab. S3).

Under warmer conditions (28 °C test temperature), *L. niger* and *L. platythorax* ants were more drought-resistant after warm acclimation, but this was not true for *L. brunneus* (acclimation $\chi^2_2 = 17.8$, $p < 0.0001$; species $\chi^2_2 = 22.0$, $p < 0.0001$; interaction $\chi^2_4 = 10.3$, $p = 0.036$). In both species, acclimation to 28 °C significantly enhanced survival compared to 20 °C acclimation. In *L. platythorax*, fluctuating acclimation resulted in a similar survival benefit, which was less pronounced in *L. niger*. To sum up, warm acclimation increased drought survival at 28 °C test temperature for *L. niger* and *L. platythorax* and at 20 °C for *L. platythorax*, but not for the other treatments (Tab. S3, Fig. S3). In all treatments and test temperatures, *L. platythorax* survived the longest, although not always significantly longer than both other species. For *L. brunneus* however, acclimation did not affect survival at all.

Overall, warm acclimation increased drought resistance, even at cooler temperatures. The acclimatory 'gain' in drought resistance was highest in *L. platythorax*, followed by *L. niger*. Only in *L. brunneus*, acclimation did not affect survival at all.

Discussion

Chemical composition: which changes match predictions, which do not?

Water loss is temperature-dependent. This is because at high temperatures, more CHCs melt, and the viscosity of liquid CHCs decreases. At the same time, water vapor pressure increases. All factors increase water loss, i.e. the diffusion of water molecules, through the cuticle. To counteract this, warm-acclimating insects increase the proportion of solid or highly viscous hydrocarbons (such as *n*-alkanes or monomethyl alkanes) at the expense of low-viscosity, early-melting hydrocarbons (such as alkadienes, dimethyl or trimethyl alkanes) (Gibbs & Pomonis 1995; Gibbs 1998; Gibbs 2002; Gibbs & Rajpurohit 2010). Such patterns have been shown in the past (Hadley 1977; Toolson & Hadley 1979; Gibbs & Mousseau 1994; Rajpurohit *et al.* 2017; Sprenger *et al.* 2018). Alternatively, or in addition, they might increase the CHC chain length, which also raises melting points (Gibbs & Pomonis 1995) and/or increase the overall CHC quantity, which reduces water diffusion through the CHC layer without changing phase behaviour. This is why in this study, we compared acclimation strategies across species, and studied their physical mechanisms as well as their actual impacts on drought resistance. Across insects, CHC profiles are usually rich either in methyl-branched alkanes (especially

dimethyl and trimethyl alkanes) or in unsaturated hydrocarbons, but rarely both (Menzel, Blaimer & Schmitt 2017; FM unpublished data). This is why we chose *L. niger* and *L. platythorax*, which are dominated by dimethyl or trimethyl alkanes, and *L. brunneus*, which is dominated by unsaturated hydrocarbons.

In our study, CHC changes of *Lasius niger* and *L. platythorax* largely confirmed the above predictions: warm-acclimated individuals had more late-melting CHCs like *n*-alkanes and monomethyl alkanes, but less early-melters like di- or trimethyl alkanes. For rarer CHC classes (abundance < 10%) this was not always found, however, possibly due to relatively higher noise at low abundances. Nonetheless, it is surprising that the dimethyl alkanes did not change in abundance in *L. platythorax* although they contributed 50% of the profile. Interestingly, absolute CHC quantities were not part of the acclimation strategy in these species, being unaffected by acclimation or even lower in warm-acclimated species.

For *L. brunneus* however, only some acclimatory changes are in line with the predictions, but others are not. Here, alkenes increased with warm acclimation, whereas methyl alkenes decreased. This makes sense if we consider that among unsaturated hydrocarbons, unbranched alkenes are those with the highest melting point, presumably much higher than methyl alkenes. However, that neither *n*-alkanes nor monomethyl alkanes were upregulated in warm-acclimated ants is unexpected, even if the *n*-alkanes increased in chain length. These two classes should provide the best waterproofing, and thus the best lever to improve waterproofing. Instead, *L. brunneus* showed higher absolute CHC quantities in the warm and especially the fluctuating treatment, which may be another (albeit here ineffective) way to reduce water loss.

Effect of temperature fluctuation

In *L. niger* and *L. platythorax*, workers from fluctuating treatments showed a CHC composition that was in between the 20 °C and the 28 °C treatment, which makes sense given that the average temperature of the fluctuating temperature was around 24 °C. In contrast, *L. brunneus* showed very different, unexpected CHC changes when acclimating to fluctuating conditions, suggesting that in this species, fluctuating conditions posed acclimatory demands that systematically differed from any constant regime. The fluctuating regime resulted in less *n*-alkanes, more alkadienes, and a lower viscosity; all these effects should actually reduce desiccation resistance. Only absolute CHC quantities were highest. As a consequence, fluctuating conditions might be more costly for *L. brunneus* than for the other species: most of the observed chemical changes should rather reduce than increase waterproofing, and upregulated CHC production might be an additional metabolic cost. This tentatively suggests that for *L. brunneus*, fluctuating conditions might be harder to cope with than for the other two ant species.

Heterogeneous phase behaviour may be adaptive

All CHC profiles of the three study species, regardless of acclimation treatment, were biphasic with liquid and solid parts at ambient temperature. Upon decreasing temperature, we often observed gelification (i.e. solidification) in some parts of the liquid phase. However, our most notable result was that we found different viscosities even within the liquid phase of the same sample. To our knowledge, this heterogeneity of the liquid phase was not reported before for cuticular hydrocarbons. It might be due to a miscibility gap, i.e. a phase separation of compounds that occurs only at certain temperatures (Jirát *et al.* 2009). Miscibility gaps have been reported from binary systems containing hydrocarbons before (Ferloni *et al.* 1971), rendering it a plausible mechanisms for CHC heterogeneity. We cannot rule out that the CHCs on insect body surfaces might form structures different from those on an object slide. To our knowledge, the structural arrangement of CHCs *in* situ, i.e. on insect bodies, has not yet been studied. CHCs are excreted on the cuticle by specialized carrier proteins (lipophorins) (Wang *et al.* 2021), but there are no reports on enzymes that manipulate structural assembly of CHCs directly on the cuticle so far. Thus, we have little reason to assume that they form any structures beyond the self-assembly that should also happen on artificial surfaces like object slides.

The picture that emerges from our study is that, at any temperature the insect can experience, CHCs are biphasic, both solid and liquid, but also that the liquid phase is heterogeneous in itself. The phase with lowest viscosity is most abundant, which is why we additionally analysed its behaviour separately here. Its viscosity ranged from 0.05 to 0.6 Pa*s in our study, similar to a previous report (0.1 to 0.4 Pa*s; Menzel *et al.* 2019). We suggest to regard this low-viscous phase as a ‘matrix’ or ‘suspending fluid’, with more viscous or solid parts floating in it. Note that the apparent homogeneity of the microrheological CHC samples at 32°C (being entirely liquid with a homogenous viscosity) might result from the collection procedure before the viscosity measurements, which does not allow the collection of solid or gelified phases. This does not affect any of our conclusions, but especially given the DSC data, it is important to keep in mind that the liquid phase is probably heterogeneous also at higher temperatures.

We hypothesize that heterogeneity of the liquid phase is beneficial for the ant. When temperature drops, certain parts solidify or become more viscous, but there is no risk that the entire layer gelifies simultaneously, which would compromise its functionality all of a sudden. Similarly, a layer that melted completely at a certain temperature would abruptly become more permeable for water, which would be detrimental for the insect as well. Thus, a heterogeneous CHC layer increases the robustness of its physical properties, thus helping to maintain homeostasis. Hence, CHC composition might experience selection for heterogeneity, at least in habitats with frequent temperature fluctuations. Note that here, heterogeneity refers to the phase behaviour and not necessarily to more complex chemical composition.

Acclimatory changes in viscosity

In *L. niger* and *L. platythorax* viscosity of the matrix did not change with acclimation treatment, despite the strong chemical changes. We hypothesize that due to phase separation, the CHC changes did not affect matrix viscosity, but rather led to either a higher abundance of more viscous parts, or higher viscosity of these parts. Unfortunately, viscosity cannot be measured for gelified parts, which is why heterogeneity of viscosity is generally hard to quantify if gelified parts are to be included.

Again, *L. brunneus* departs from the other two species, being the only one where the matrix viscosity changed with acclimation. This species seemed more homogenous in our analyses, which might limit its ability to acclimate, and indeed did not show acclimatory survival benefits. Viscosity was highest in cool-acclimated workers, and lowest for those from the fluctuating treatment. Here, viscosity and CHC composition can tentatively be linked: in total, the fluctuating treatment (which was least viscous) contained most fluid compounds (alkenes, alkadienes and methyl-branched alkenes), followed by the 28°C and the 20 °C treatment. In turn, the sum of solid to highly viscous CHCs (*n*-alkanes and monomethyl alkanes) was highest in the 20°C treatment and lowest in the fluctuating treatment (Fig. 3). Assuming a more homogenous mixture than in the other two species, these effects may explain the observed viscosities.

Melting ranges

Like viscosity, melting ranges of *L. niger* and *L. platythorax* were relatively similar, which is surprising given their strong chemical differences. Given this, it is hard to assign certain melting ranges to chemical compounds. The melting ranges showed much fewer individual peaks than one would expect given the high number of compounds. This indicates that different hydrocarbon molecules interact tightly to form continuous melting ranges rather than a high number of melting peaks (Menzel *et al.* 2019). This effect should be adaptive because continuous melting makes the CHC layer more robust against temperature fluctuations than sudden melting of larger CHC quantities.

The most prominent acclimation-induced melting peaks (between 30 and 50 °C in *L. niger*) are likely caused by *n*-alkanes and/or terminally branched monomethyl alkanes. Pure *n*-alkanes of the relevant chain lengths (*n*-C25 to *n*-C33) melt between 54 and 71 °C (Lide 2008). Interestingly though, there was no relevant melting detectable beyond 50 °C. Albeit melting detection is affected by the heating rate during DSC, this result suggests that in the CHC mixture, n-alkanes melted earlier due to hindered packing of the molecules compared to the pure substances. This effect becomes especially pronounced in complex mixtures with many molecules of similar chemical structure (e.g. long hydrocarbon chains with no or only few branches and kinks). In that case, the molecules mix well, so that areas of 'pure' substances can become very small. As a consequence, intermolecular interactions are weaker and melting transitions can occur at lower temperatures. Demixing can occur in liquid phases due to diffusion if left for equilibration, but the kinetics are usually much slower than the experimentally

applied timeframes (as e.g. the time needed for one DSC measurement). This scenario links the two observations that *n*-alkanes were more abundant in warm-acclimated *L. niger* compared to the other treatments, but also to *L. platythorax*, and that the same is true for melting proportions in the range of 30 to 50 °C.

One main new insight from our melting data is that adaptive warm acclimation does not necessarily need more solid compounds – this is shown by the surprisingly few compounds melting between 20 and 28 °C. Hence, waterproofing is also possible by the liquid phase if it is viscous enough.

Drought Survival

In two of three ant species, acclimation led to increased drought resistance. This effect was most pronounced at 28 °C, but much weaker at 20 °C test temperature. While this was expected given that water permeability increases with temperature due to CHC melting and increased water vapour pressure, it shows that drought survival should always be measured at multiple temperatures. An earlier study found consistent effects of test temperature on the drought survival of springtails (Chown *et al.* 2007) Notably, even at 20 °C, the 20 °C-acclimated workers did not survive better than the 28 °C-acclimated ones, which corroborates our assumption that mortality was driven by water loss. It also confirms that acclimatory CHC changes are not only to optimise desiccation resistance – if this was true, ants would always have a 'warm-acclimated' profile. Thus, this is evidence that CHC profiles are also constrained by the need to remain fluid to some degree, probably for communication or other purposes (Menzel *et al.* 2019).

In *L. niger* and *L. platythorax*, warm acclimation and – for *L. platythorax* – also fluctuating acclimation – significantly increased survival at 28 °C test temperature (Fig. S3). Although *L. brunneus* was the only species with viscosity changes during acclimation, its survival was unaffected by acclimation. However, it is possible (albeit unlikely) that in *L. brunneus*, acclimation and survival might also have been affected by keeping them in smaller worker groups without brood compared to the other two species.

In *L. niger*, the higher survival rates of warm-acclimated workers can be linked to an increase in solid CHCs (*n*-alkanes and possibly monomethyl alkanes), i.e. those that melted above 28 °C (Gibbs & Rajpurohit 2010). Since viscosity is only defined for liquids, this effect did not impact viscosity. Water loss has been linked to acclimation and chemical changes before (Hadley 1977; Gibbs & Mousseau 1994; Rajpurohit *et al.* 2017). However, most studies focused on *n*-alkane abundance or CHC chain length. As shown here, changes in other compounds are similarly important for waterproofing, as exemplified by *L. platythorax*, which showed clear acclimatory survival benefits but hardly possesses *n*-alkanes.

Acclimatory strategies

The three ants we studied use different acclimatory strategies, i.e. different levers to achieve higher waterproofing. *Lasius niger* had the most intuitive strategy: warm-acclimated ants produced more, and longer *n*-alkanes, and hence more solid compounds. Indeed, this corresponded to more CHCs melting above 30 °C, and a longer survival of warm-acclimated workers. For *L. platythorax*, the picture is less straightforward. Warm acclimation did not result in more (nor longer) *n*-alkanes, and there was no increase in CHCs melting above 30°C. We hypothesize that *L. platythorax* acclimates to warmer climates by upregulating CHCs that melt between 10 and 20 °C (presumably monomethyl alkanes). These compounds are liquid above 20 °C, but more viscous than the matrix, and hence can reduce water permeability. This strategy seems to be also used by *L. niger*. Warm-acclimated *L. niger* also upregulated monomethyl alkane production; and the liquid parts of their CHC layers were similarly heterogeneous (Fig. 7B). Unfortunately, the viscosity of highly viscous phases is hard to quantify, as we are approaching the detection limit of Brownian motion. Therefore, a large proportion of the tracer beads in this phase cannot be used to quantify the heterogeneity of the sample. For *L. brunneus*, the acclimatory changes are hardest to explain, since several chemical changes should rather increase than decrease water loss. The CHC profile of this species is more homogenous, which explains why the viscosity of the matrix changed with acclimation. Here, considering the changes that should enhance drought resistance, warm acclimation seemed to take place mostly by higher overall CHC production and higher average *n*-alkane chain length than by compositional changes in substance classes. However, since for *L. brunneus* acclimation did not result in higher survival, it is unclear whether the observed changes are actually adaptive. The arboreal *L. brunneus* usually nests in the wood or bark of living trees. Thus, the desiccation pressure might be substantially lower than in *L. niger* and *L. platythorax* because even during droughts, its nests should receive some humidity through the tree's xylem. The lower drought survival of this species hence might be linked to a lower desiccation pressure due to its arboreal lifestyle.

Conclusions: cuticular hydrocarbons as a functional trait

Functional traits are defined as measurable traits that vary across species and affect the organism's fitness (McGill *et al.* 2006). As shown here, cuticular hydrocarbon profiles can be seen as a functional trait with multiple dimensions. They show strong qualitative differences among species, e.g. concerning their content in unsaturated hydrocarbons. This is related to their ecological niche, because unsaturated compounds are especially common in species from wet habitats (Martin, Helanterae & Drijfhout 2008; Van Wilgenburg, Symonds & Elgar 2011; Menzel, Blaimer & Schmitt 2017), and CHC changes affect fitness. To understand these fitness affects, we studied here how CHC composition translates to the physical mechanism of waterproofing, and the ants' ability to enhance drought resistance via acclimation. Although generalisations must be regarded with caution at this

stage, it seems possible that profiles rich in methylbranched alkanes are more heterogeneous, which helps to deal with temperature fluctuations.

Future studies should test how much our results can be generalised across species to better understand the link between CHC composition, acclimation strategy, and the ability to acclimate. Here, we need to include further parameters of the CHC profile relevant for waterproofing. Among others, these include average chain length and *n*-alkane content. Several earlier studies (Gibbs, Mousseau & Crowe 1991; Gibbs & Mousseau 1994; Gibbs, Chippindale & Rose 1997) showed that they are highly relevant, but they do not tell the entire story, especially in species with only few *n*-alkanes. Here, multi-species comparisons of physical properties will help us to establish a model on phase behaviour and inter-molecular interactions between different hydrocarbons on the insect cuticle (Krupp *et al.* 2020; Blomquist & Ginzel 2021). Further research may then enable us to predict an organism's ability to acclimate and to cope with certain ecological conditions based on its CHC profile.

Acknowledgements

We thank the Obere Naturschutzbehörde (SGD Süd, Thomas Schlindwein) and Jürgen Koch (forest district Ober-Olm) for permission to collect ants at the Ober-Olmer Wald (permission no. 42/553-254/287-19). Furthermore, we are grateful to Petra Räder for the DSC measurements.

Competing interests

The authors declare no conflict of interest.

Funding

This study was funded by a Heisenberg fellowship of the German Research Foundation (DFG) to Florian Menzel (grant no. ME 3842/6-1). Furthermore, it was supported by the German National Exchange Service (DAAD, PPP Procope France, project ID: 57388961, to FM) with funds from the Federal Ministry of Education and Research (Bundesministerium für Bildung und Forschung). BA was supported by PHC Procope 2018 (project ID: 40427NM) with funds from MEAE (Ministère de l'Europe et des Affaires étrangères) and MESRI (Ministère de l'Enseignement Supérieur, de la Recherche et de l'Innovation).

Data availability

All raw data will be uploaded as online supplement or on Dryad upon acceptance of the paper.

Author contributions

FM conceived the study; MW and LB collected the ants, conducted the acclimation treatments and collected the chemical data; BA and LB collected the microrheological data; SM collected the DSC data; LB, BA, SM and FM wrote the paper. All authors approved the final version of the manuscript.

References

Abou, B., Gay, C., Laurent, B., Cardoso, O., Voigt, D., Peisker, H. & Gorb, S. (2010) Extensive collection of femtolitre pad secretion droplets in the beetle Leptinotarsa decemlineata allows nanolitre microrheology. *Journal of The Royal Society Interface,* **7,** 1745-1752.

Bates, D., Maechler, M., Bolker, B., Walker, S., Christensen, R.H.B., Singmann, H., Dai, B., Scheipl, F. & Grothendieck, G. (2011) Package 'lme4'. *Linear mixed-effects models using S4 classes. R package version,* **1**.

Blomquist, G. & Bagnères, A.-G. (2010) Introduction: history and overview of insect hydrocarbons. *Insect hydrocarbons: biology, biochemistry, and chemical ecology***,** 3-18.

Blomquist, G.J. & Bagnéres, A. (2010) Structure and analysis of insect hydrocarbons. *Insect hydrocarbons: biology, biochemistry, and chemical ecology***,** 19-34.

Blomquist, G.J. & Ginzel, M.D. (2021) Chemical ecology, biochemistry, and molecular biology of insect hydrocarbons. *Annual Review of Entomology,* **66,** 45-60.

Buellesbach, J., Whyte, B.A., Cash, E., Gibson, J.D., Scheckel, K.J., Sandidge, R. & Tsutsui, N.D. (2018) Desiccation resistance and micro-climate adaptation: cuticular hydrocarbon signatures of different Argentine ant supercolonies across California. *Journal of Chemical Ecology,* **44,** 1101-1114.

Chown, S.L., Slabber, S., McGeoch, M.A., Janion, C. & Leinaas, H.P. (2007) Phenotypic plasticity mediates climate change responses among invasive and indigenous arthropods. *Proceedings of the Royal Society B: Biological Sciences,* **274,** 2531-2537.

Chown, S.L., Sørensen, J.G. & Terblanche, J.S. (2011) Water loss in insects: an environmental change perspective. *Journal of Insect Physiology,* **57,** 1070-1084.

Colinet, H., Sinclair, B.J., Vernon, P. & Renault, D. (2015) Insects in fluctuating thermal environments. *Annual Review of Entomology,* **60,** 123-140.

Cooper, R., Lee, H., González, J.M., Butler, J., Vinson, S.B. & Liang, H. (2008) Lubrication and Surface Properties of Roach Cuticle. *Journal of Tribology,* **131**.

De Guzmán, J. (1913) Relación entre la Fluidez y el Calor de Fusion. *An. Soc. Esp. Fis. Quim,* **11,** 353-362.

Drechsler, P. & Federle, W. (2006) Biomechanics of smooth adhesive pads in insects: influence of tarsal secretion on attachment performance. *Journal of comparative physiology,* **2006 v.192 no.11,** pp. 1213-1222.

Einstein, A. (1905) Über die von der molekularkinetischen Theorie der Wärme geforderte Bewegung von in ruhenden Flüssigkeiten suspendierten Teilchen. *Annalen der physik,* **17,** 549-560.

Eyring, H. (1935) The activated complex in chemical reactions. *The Journal of Chemical Physics,* **3,** 107-115.

Ferloni, P., Geangu-Moisin, A., Franzosini, P. & Rolla, M. (1971) Binary Systems Containing Hydrocarbons IV. Miscibility Gaps in 18 Nitromethane+ 1-, 2-, 3-and 4-alkenes. *Zeitschrift für Naturforschung A,* **26,** 1713-1716.

Ferveur, J.-F. & Cobb, M. (2010) Behavioral and evolutionary roles of cuticular hydrocarbons in Diptera. *Insect hydrocarbons: biology, biochemistry and chemical ecology***,** 325-343.
Fox, J., Weisberg, S., Adler, D., Bates, D., Baud-Bovy, G., Ellison, S., Firth, D., Friendly, M., Gorjanc, G. & Graves, S. (2012) Package 'car'. *Vienna: R Foundation for Statistical Computing***,** 16.
Gibbs, A. & Mousseau, T.A. (1994) Thermal acclimation and genetic variation in cuticular lipids of the lesser migratory grasshopper (Melanoplus sanguinipes): effects of lipid composition on biophysical properties. *Physiological Zoology*, **67,** 1523-1543.
Gibbs, A., Mousseau, T.A. & Crowe, J.H. (1991) Genetic and acclimatory variation in biophysical properties of insect cuticle lipids. *Proceedings of the National Academy of Sciences*, **88,** 7257-7260.
Gibbs, A. & Pomonis, J.G. (1995) Physical properties of insect cuticular hydrocarbons: The effects of chain length, methyl-branching and unsaturation. **112,** 243-249.
Gibbs, A.G. (1998) Water-proofing properties of cuticular lipids. *American Zoologist*, **38,** 471-482.
Gibbs, A.G. (2002) Lipid melting and cuticular permeability: new insights into an old problem. *Journal of Insect Physiology*, **48,** 391-400.
Gibbs, A.G., Chippindale, A.K. & Rose, M.R. (1997) Physiological mechanisms of evolved desiccation resistance in Drosophila melanogaster. *The Journal of Experimental Biology*, **200,** 1821-1832.
Gibbs, A.G. & Rajpurohit, S. (2010) Cuticular lipids and water balance. *Insect hydrocarbons: biology, biochemistry, and chemical ecology***,** 100-120.
Hadley, N.F. (1977) Epicuticular lipids of the desert tenebrionid beetle, Eleodes armata: seasonal and acclimatory effects on composition. *Insect Biochemistry*, **7,** 277-283.
Hartke, J., Sprenger, P.P., Sahm, J., Winterberg, H., Orivel, J., Baur, H., Beuerle, T., Schmitt, T., Feldmeyer, B. & Menzel, F. (2019) Cuticular hydrocarbons as potential mediators of cryptic species divergence in a mutualistic ant association. *Ecology and evolution*, **9,** 9160-9176.
Jirát, J., Košata, B., Jenkins, A. & McNaught, A. (2009) IUPAC: Research Triagle Park. NC.
Kather, R. & Martin, S.J. (2012) Cuticular hydrocarbon profiles as a taxonomic tool: advantages, limitations and technical aspects. *Physiological Entomology*, **37,** 25-32.
Kather, R. & Martin, S.J. (2015) Evolution of cuticular hydrocarbons in the hymenoptera: a meta-analysis. *Journal of Chemical Ecology*, **41,** 871-883.
Kellermann, V., Loeschcke, V., Hoffmann, A.A., Kristensen, T.N., Fløjgaard, C., David, J.R., Svenning, J.C. & Overgaard, J. (2012) PHYLOGENETIC CONSTRAINTS IN KEY FUNCTIONAL TRAITS BEHIND SPECIES'CLIMATE NICHES: PATTERNS OF DESICCATION AND COLD RESISTANCE ACROSS 95 DROSOPHILA SPECIES. *Evolution: International Journal of Organic Evolution*, **66,** 3377-3389.
Krupp, J.J., Nayal, K., Wong, A., Millar, J.G. & Levine, J.D. (2020) Desiccation resistance is an adaptive life-history trait dependent upon cuticular hydrocarbons, and influenced by mating status and temperature in D. melanogaster. *Journal of Insect Physiology*, **121,** 103990.
Leonhardt, S.D., Menzel, F., Nehring, V. & Schmitt, T. (2016) Ecology and evolution of communication in social insects. *Cell*, **164,** 1277-1287.
Lide, D.R. (2008) CRC Handbook of Chemistry and Physics CRC. *Boca Raton*.
Maroncelli, M., Qi, S.P., Strauss, H.L. & Snyder, R.G. (1982) Nonplanar conformers and the phase behavior of solid n-alkanes. *Journal of the American Chemical Society*, **104,** 6237-6247.
Martin, S.J., Helanterae, H. & Drijfhout, F.P. (2008) Evolution of species-specific cuticular hydrocarbon patterns in Formica ants. *Biological Journal of the Linnean Society*, **95,** 131-140.
McGill, B.J., Enquist, B.J., Weiher, E. & Westoby, M. (2006) Rebuilding community ecology from functional traits. *Trends in ecology & evolution*, **21,** 178-185.
Menzel, F., Blaimer, B.B. & Schmitt, T. (2017) How do cuticular hydrocarbons evolve? Physiological constraints and climatic and biotic selection pressures act on a complex functional trait. *Proceedings of the Royal Society B: Biological Sciences*, **284,** 20161727.
Menzel, F., Morsbach, S., Martens, J.H., Räder, P., Hadjaje, S., Poizat, M. & Abou, B. (2019) Communication versus waterproofing: the physics of insect cuticular hydrocarbons. *Journal of Experimental Biology*, **222**.
Menzel, F., Zumbusch, M. & Feldmeyer, B. (2018) How ants acclimate: impact of climatic conditions on the cuticular hydrocarbon profile. *Functional Ecology*, **32,** 657-666.

Michelutti, K.B., Soares, E.R.P., Sguarizi-Antonio, D., Piva, R.C., Súarez, Y.R., Cardoso, C.A.L. & Antonialli-Junior, W.F. (2018) Influence of temperature on survival and cuticular chemical profile of social wasps. *Journal of Thermal Biology*, **71,** 221-231.

Oksanen, J., Blanchet, F.G., Kindt, R., Legendre, P., Minchin, P.R., O'hara, R., Simpson, G.L., Solymos, P., Stevens, M.H.H. & Wagner, H. (2013) Package 'vegan'. *Community ecology package, version*, **2,** 1-295.

Pokorny, T., Lunau, K., Quezada-Euan, J.J.G. & Eltz, T. (2014) Cuticular hydrocarbons distinguish cryptic sibling species in Euglossa orchid bees. *Apidologie*, **45,** 276-283.

Rajpurohit, S., Hanus, R., Vrkoslav, V., Behrman, E.L., Bergland, A.O., Petrov, D., Cvačka, J. & Schmidt, P.S. (2017) Adaptive dynamics of cuticular hydrocarbons in Drosophila. *Journal of Evolutionary Biology*, **30,** 66-80.

Seifert, B. (2008) The ants of Central European tree canopies (Hymonoptera: Formicidae)-an underestimated population? *Canopy arthropod research in Europe***,** 157-173.

Spicer, M.E., Stark, A.Y., Adams, B.J., Kneale, R., Kaspari, M. & Yanoviak, S.P. (2017) Thermal constraints on foraging of tropical canopy ants. *Oecologia*, **183,** 1007-1017.

Sprenger, P. & Menzel, F. (2020) Cuticular hydrocarbons in ants (Hymenoptera: Formicidae) and other insects: how and why they differ among individuals, colonies, and species. *Myrmecological News*, **30**.

Sprenger, P.P., Burkert, L.H., Abou, B., Federle, W. & Menzel, F. (2018) Coping with the climate: cuticular hydrocarbon acclimation of ants under constant and fluctuating conditions. *Journal of Experimental Biology*, **221**.

Steiger, S. & Stökl, J. (2014) The role of sexual selection in the evolution of chemical signals in insects. *Insects*, **5,** 423-438.

Toolson, E.C. & Hadley, N.F. (1979) Seasonal effects on cuticular permeability and epicuticular lipid composition inCentruroides sculpturatus ewing 1928 (Scorpiones: Buthidae). *Journal of comparative physiology*, **129,** 319-325.

Van Wilgenburg, E., Symonds, M. & Elgar, M. (2011) Evolution of cuticular hydrocarbon diversity in ants. *Journal of Evolutionary Biology*, **24,** 1188-1198.

Wang, Y., Ferveur, J. F., & Moussian, B. (2021). Eco- genetics of desiccation resistance in Drosophila. *Biological Reviews*, **96**, 1421-1440.

Wittke, M., Baumgart, L. & Menzel, F. (2022) Cuticular hydrocarbons in insects: Interference of communication and waterproofing in a multifunctional trait. *Functional Ecology*, in press.

Figures and Table

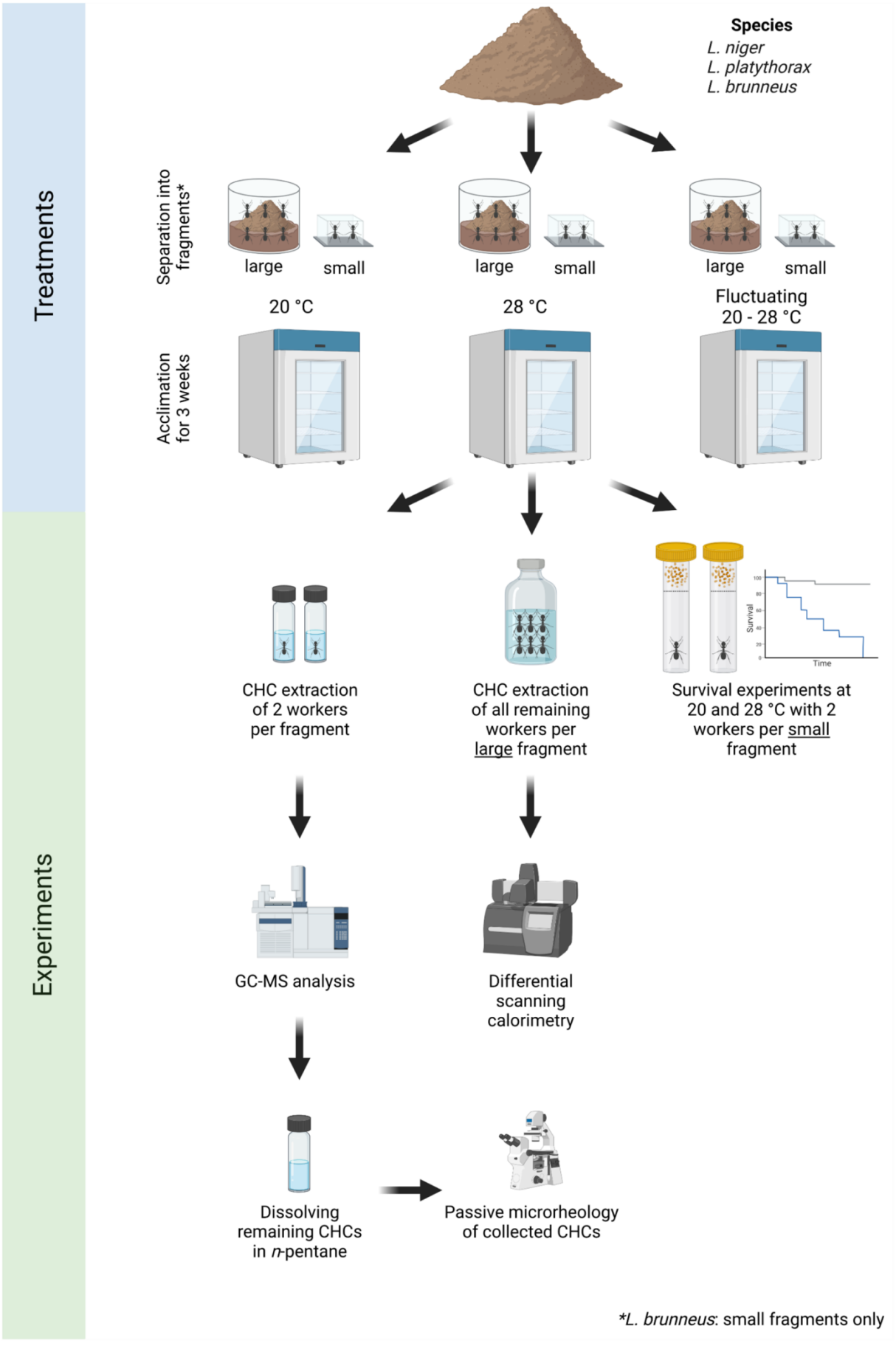

Figure 1 Graphical overview of the experimental treatments and methods used. The division into small and large fragments was made because the colonies were used simultaneously for another study (Wittke, Baumgart & Menzel 2022). The image was created with BioRender.com.

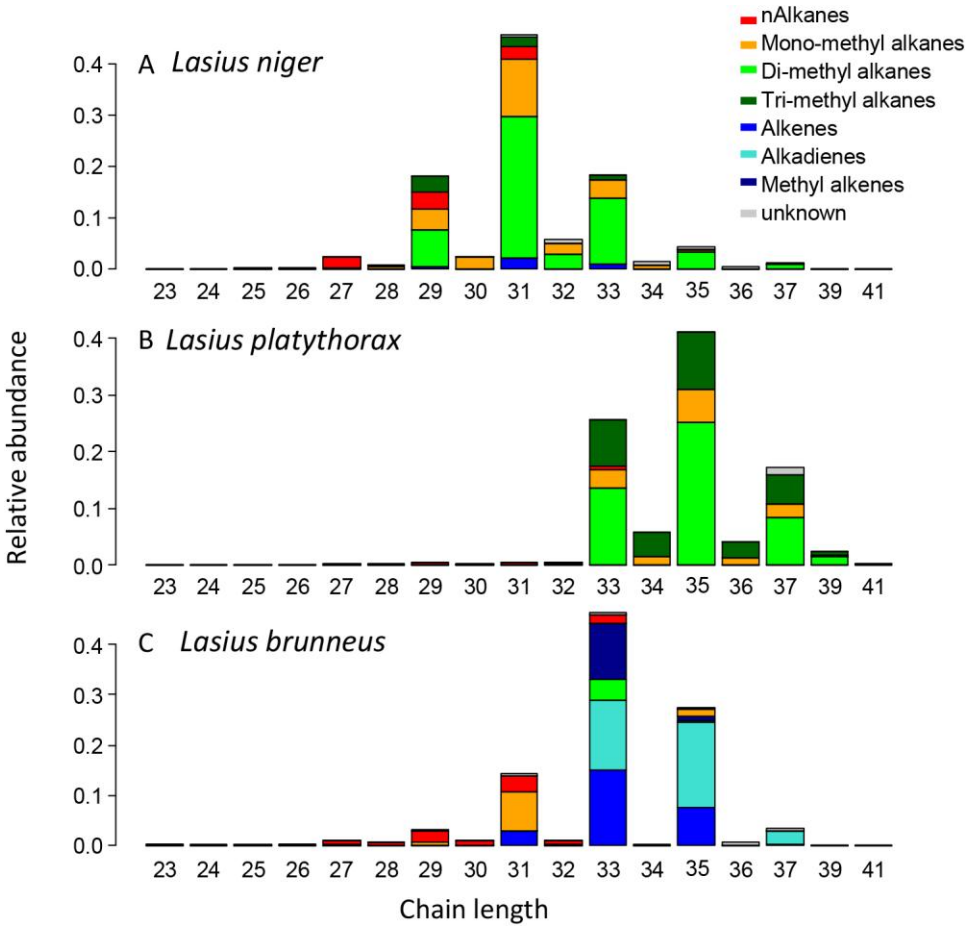

Figure 2 Visualisation of the cuticular hydrocarbon profiles of the three ant species. The x axis denotes chain length of the cuticular hydrocarbons; the bars represent the relative abundance of each CHC class per chain length and add up to 1.

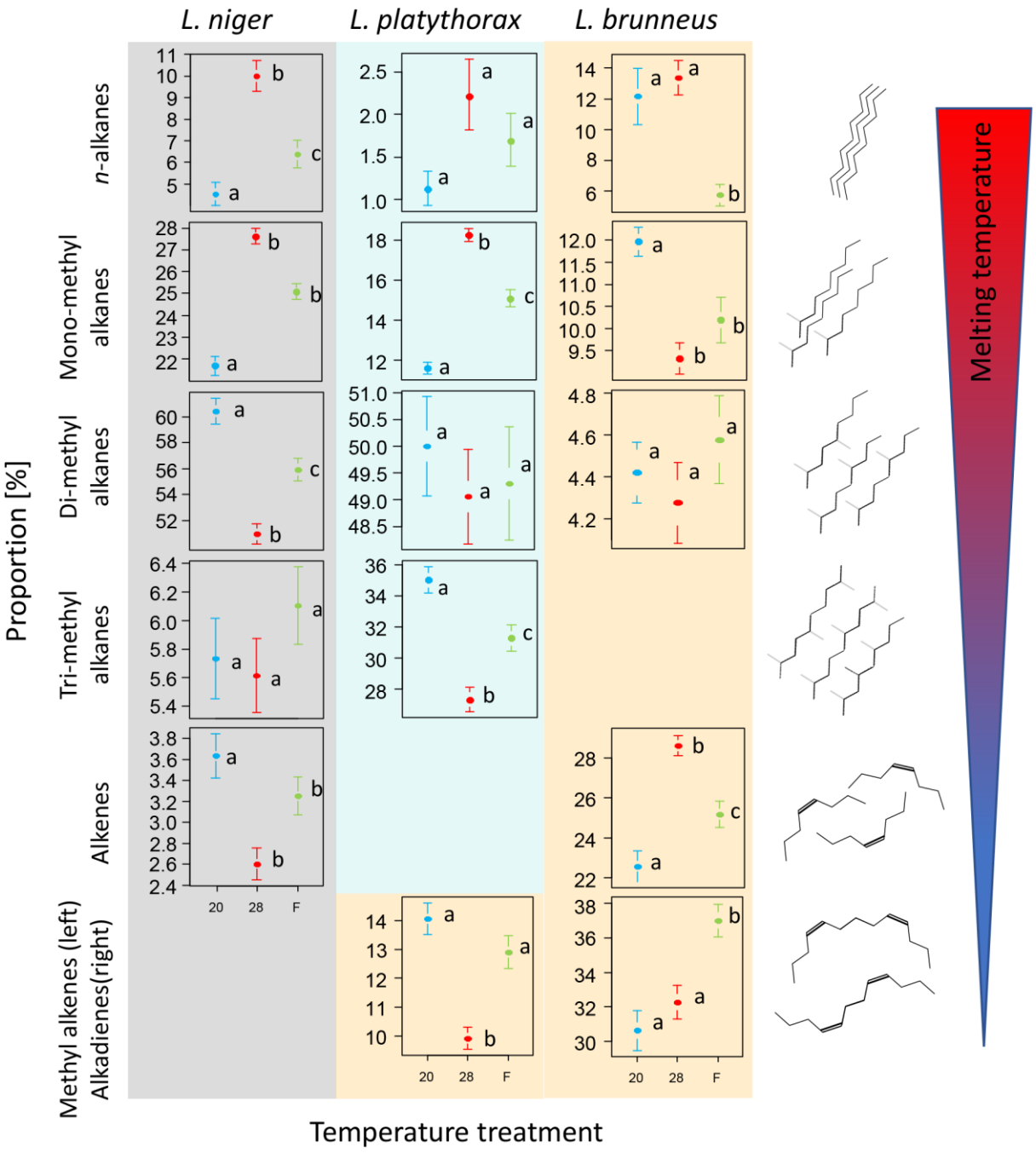

Figure 3 Acclimatory differences of the relative abundances of each CHC class. From top to bottom, the classes are sorted in decreasing melting temperature. To the right of each row, small molecules visualise the characteristics of each substance class. The graphs show proportion (mean and standard error) for the three acclimation treatments (20 °C: blue; 28 °C: red; fluctuating: green). The bottom row contains graphs of two CHC classes that only occurred in *L. brunneus*, i.e. methyl-branched alkenes and alkadienes. Plots with same letters are not significantly different according to linear mixed-effects models.

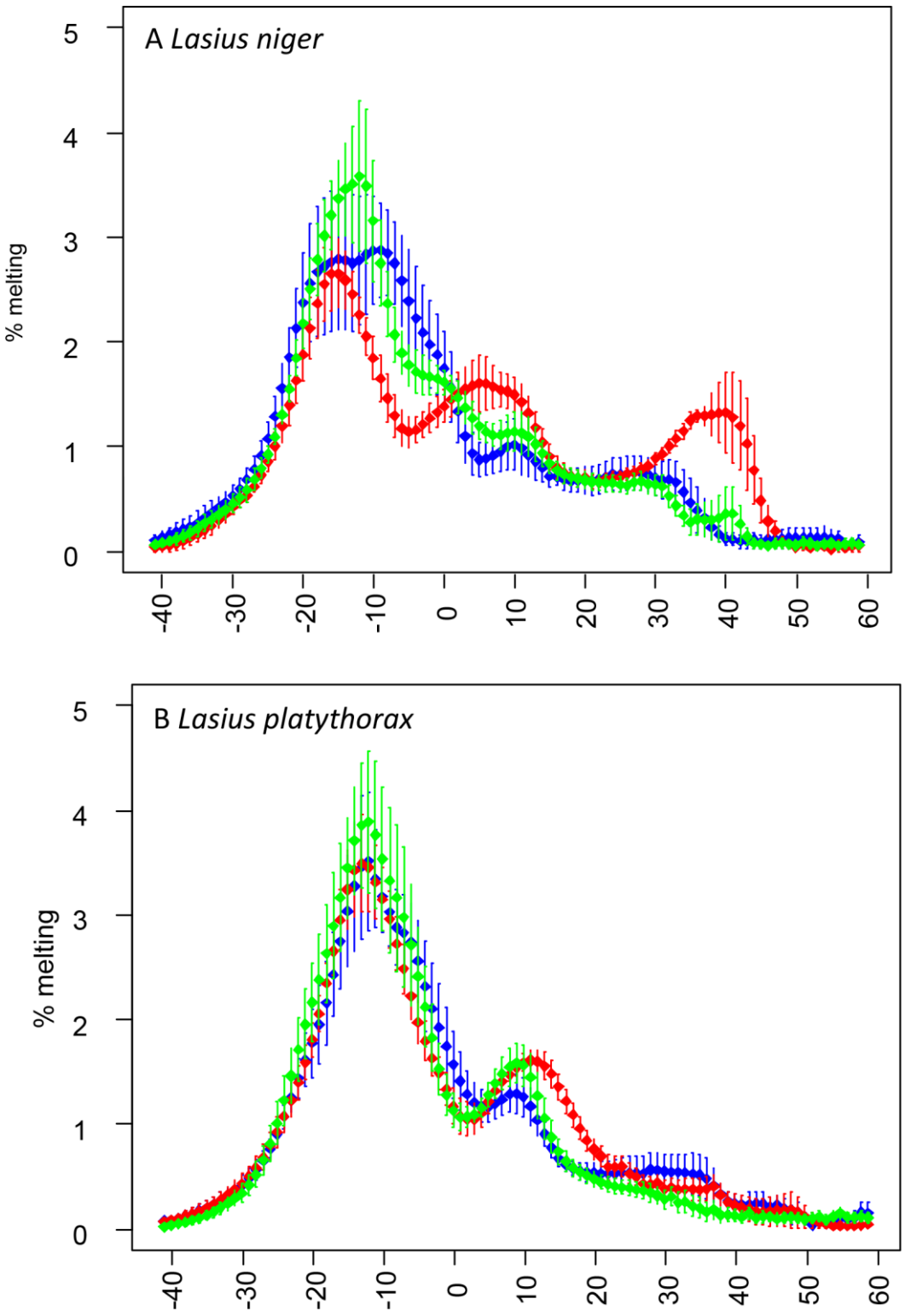

Figure 4 Melting ranges of CHC layers of *Lasius niger* and *L. platythorax*. The plots show the average (± standard error) proportion of the CHC layer that melted in each 1 K interval, separately for 20 °C acclimation (blue), 28 °C acclimation (red), and fluctuating acclimation (green).

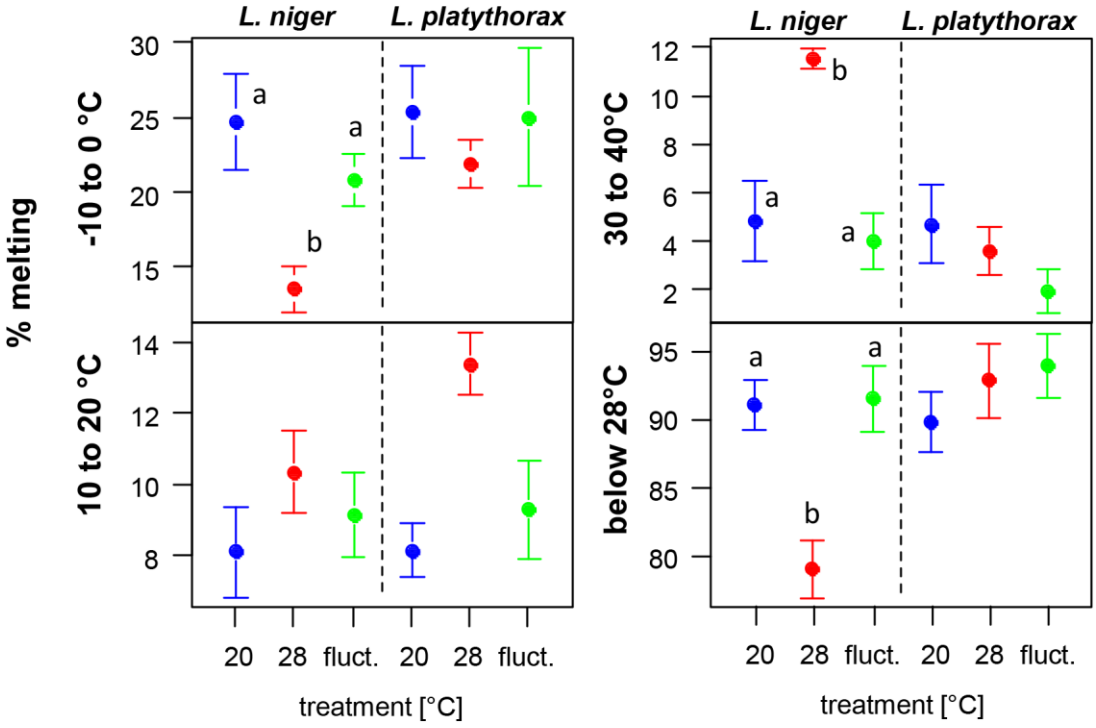

Figure 5 CHC melting in certain temperature intervals. The plots show the proportion of the CHC layer that melted in the temperature intervals -10 to 0 °C, 10 to 20 °C, and 30 to 40 °C, visualising means and standard errors. Plots with same letters are not significantly different according to linear models; we did not add letters if there were no significant differences. For the 10 – 20 °C interval, significantly more CHCs melted in 28 °C-acclimated ants compared to both other treatments; this was true for both species pooled.

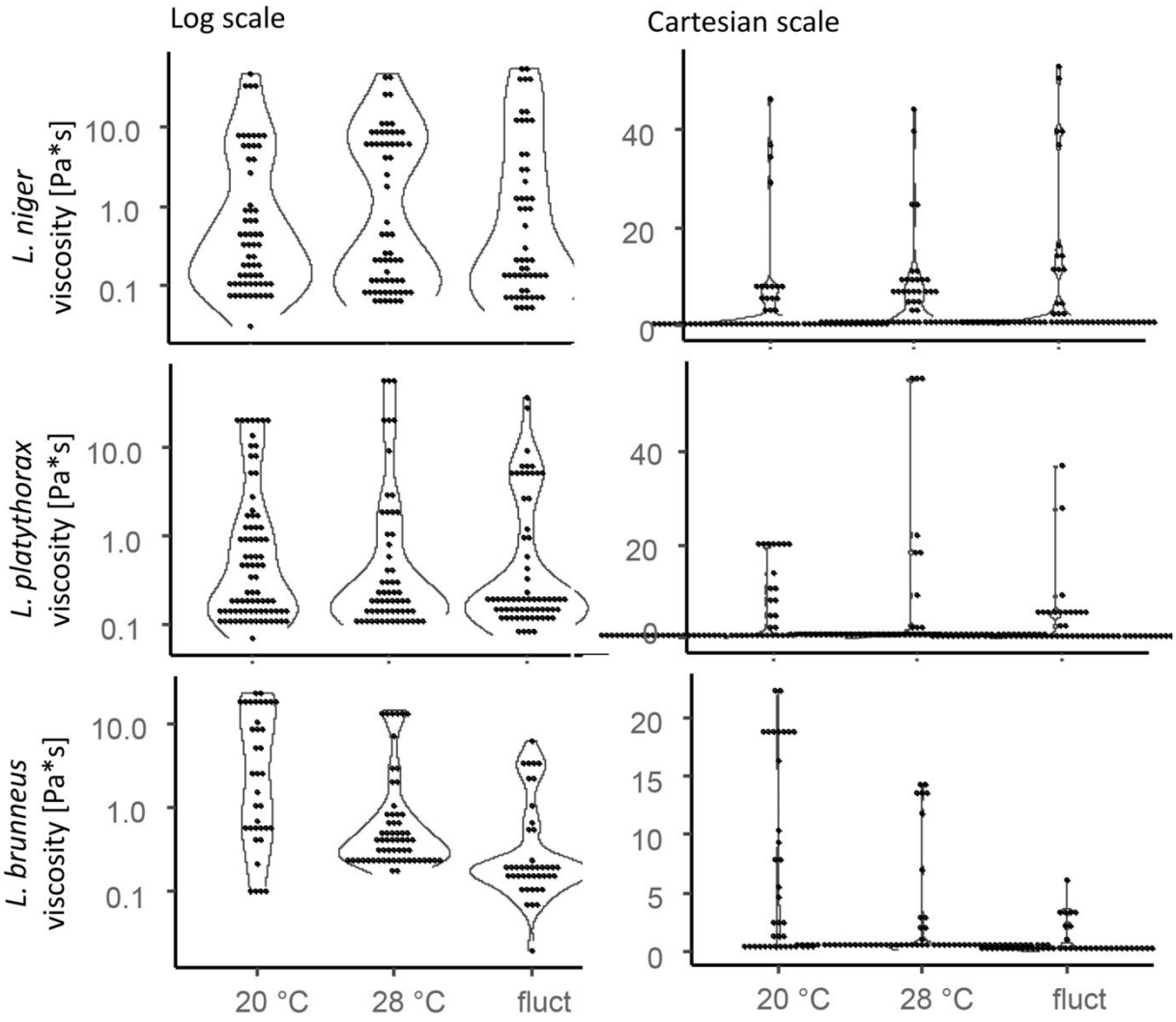

Figure 6 Viscosity of CHC layers. The violin plots show viscosities of each bead measured at 24 °C, pooled for all samples of a species and acclimation treatment. They are to visualise the distribution of viscosity values in all CHC layers measured. The data are shown once on a logarithmic scale (left) and once on a Cartesian scale (right).

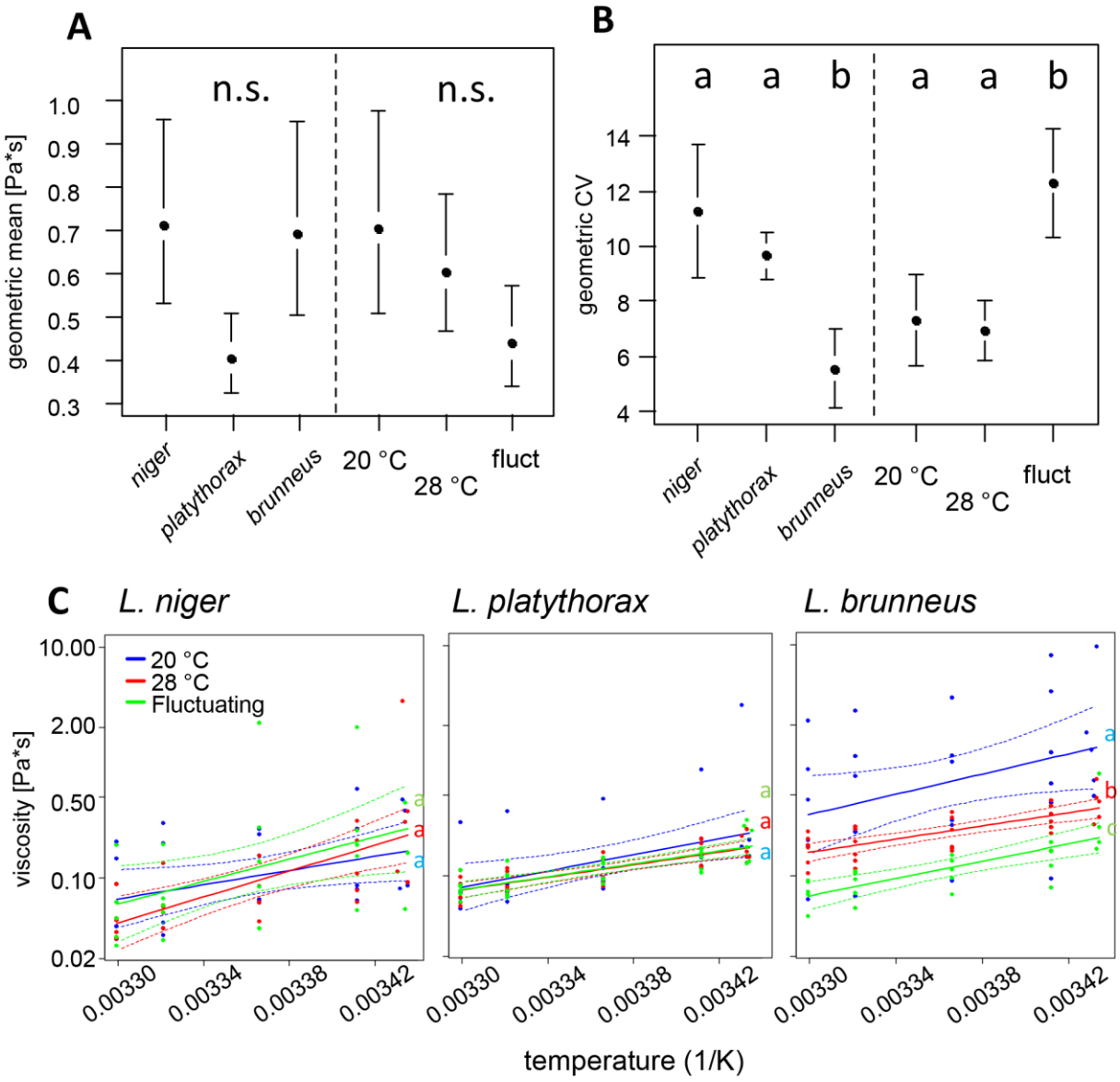

Figure 7 Viscosities of CHC layers. (A) geometric mean of all measured beads per sample, shown separated by species (left) and by acclimation treatment (right). (B) geometric coefficient of variation of all measured beads per sample, also shown per species and per acclimation treatment. (A) and (B) show means and standard error. (C) viscosity of the phase with lowest viscosity ('matrix') depending on species, acclimation treatment and measurement temperature. The graphs show Arrhenius plots: the log-transformed viscosity is plotted against inverse temperature. Here, we plotted regression lines and 95% confidence intervals based on linear models. Plots with same letters are not significantly different according to these models.

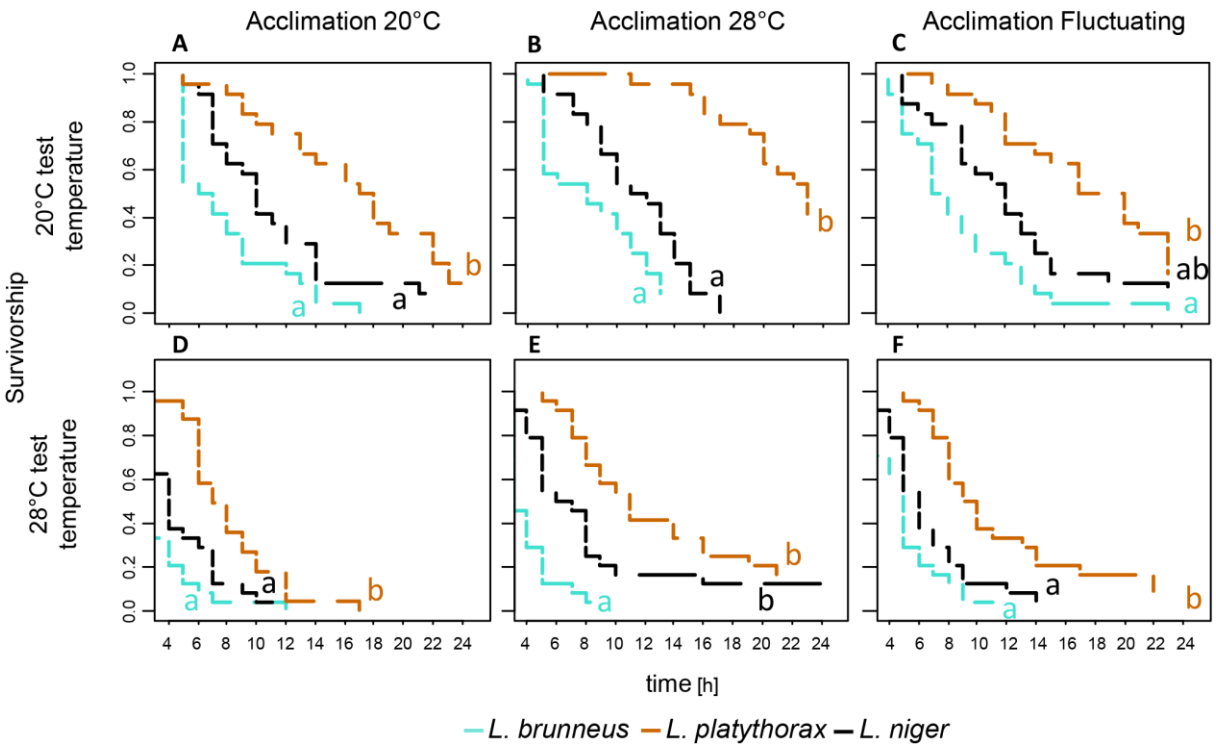

Figure 8 Drought survival of the three ant species according to different temperatures. The plots show survival curves, separately for each test temperature (20 °C or 28 °C), species, and acclimation temperature (20 °C, 28 °C or fluctuating conditions). Plots with same letters are not significantly different according to Cox mixed-effects models.

Table 1 Statistical differences of CHC classes between acclimation regimes. The factor 'acclimation' has 2 degrees of freedom in each model. See Table S1 for further statistical results. In the first two sections, all three acclimation treatments differ from each other unless noted otherwise.

class	species	average proportion	chi^2	p	Transformation used
20 °C < fluct < 28 °C					
n-alkanes*	*L. niger*	7.67 ± 0.44 %	56.59	<0.0001	arcsin-sqrt
monomethyl	*L. niger*	24.89 ± 0.3 %	156.8	<0.0001	none
monomethyl	*L. platythorax*	14.92 ± 0.31 %	228.1	<0.0001	none
alkenes	*L. brunneus*	25.82 ± 0.47 %	60.36	<0.0001	none
28 °C < fluct < 20 °C					
dimethyl alkanes	*L. niger*	55.63 ± 0.6 %	97.6	<0.0001	none
trimethyl alkanes	*L. platythorax*	31.26 ± 0.55 %	174.7	<0.0001	none
alkenes**	*L. niger*	3.15 ± 0.11 %	22.8	<0.0001	none
no treatment effects					
dimethyl alkanes	*L. platythorax*	49.47 ± 0.55 %	1.6	0.45	none
trimethyl alkanes	*L. niger*	5.82 ± 0.16 %	3.9	0.14	sqrt
n-alkanes	*L. platythorax*	2.3 ± 0.23 %	15.73	0.00038	sqrt
dimethyl alkanes	*L. brunneus*	4.42 ± 0.11 %	1.5	0.47	log
other patterns					
n-alkanes***	*L. brunneus*	10.5 ± 0.81 %	35.405	<0.0001	arcsin-sqrt
monomethyl**	*L. brunneus*	10.33 ± 0.27 %	29.14	<0.0001	arcsin-sqrt
methyl alkenes*	*L. brunneus*	12.04 ± 0.35 %	61.7	<0.0001	none
alkadienes***	*L. brunneus*	33.41 ± 0.66 %	23.14	<0.0001	none

*20 °C and *fluctuating* not significantly different; **28 °C and *fluctuating* not significantly different; ***20 °C and 28 °C not significantly different

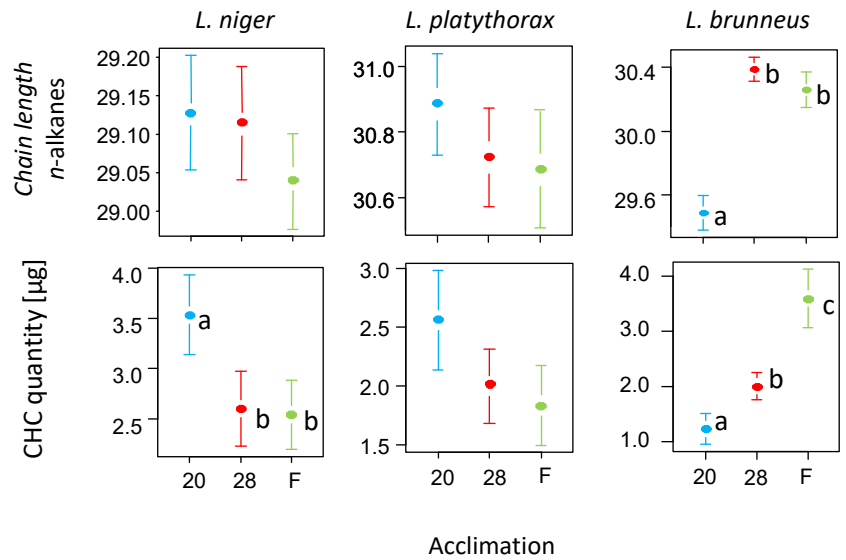

Fig. S1. Acclimatory differences of further CHC traits. Average chain length of *n*-alkanes, and absolute CHC quantity in µg. The graphs show means and standard errors for the three acclimation treatments (20°C: blue; 28°C: red; fluctuating: green). Plots with same letters (or without letters) are not significantly different according to linear mixed-effects models.

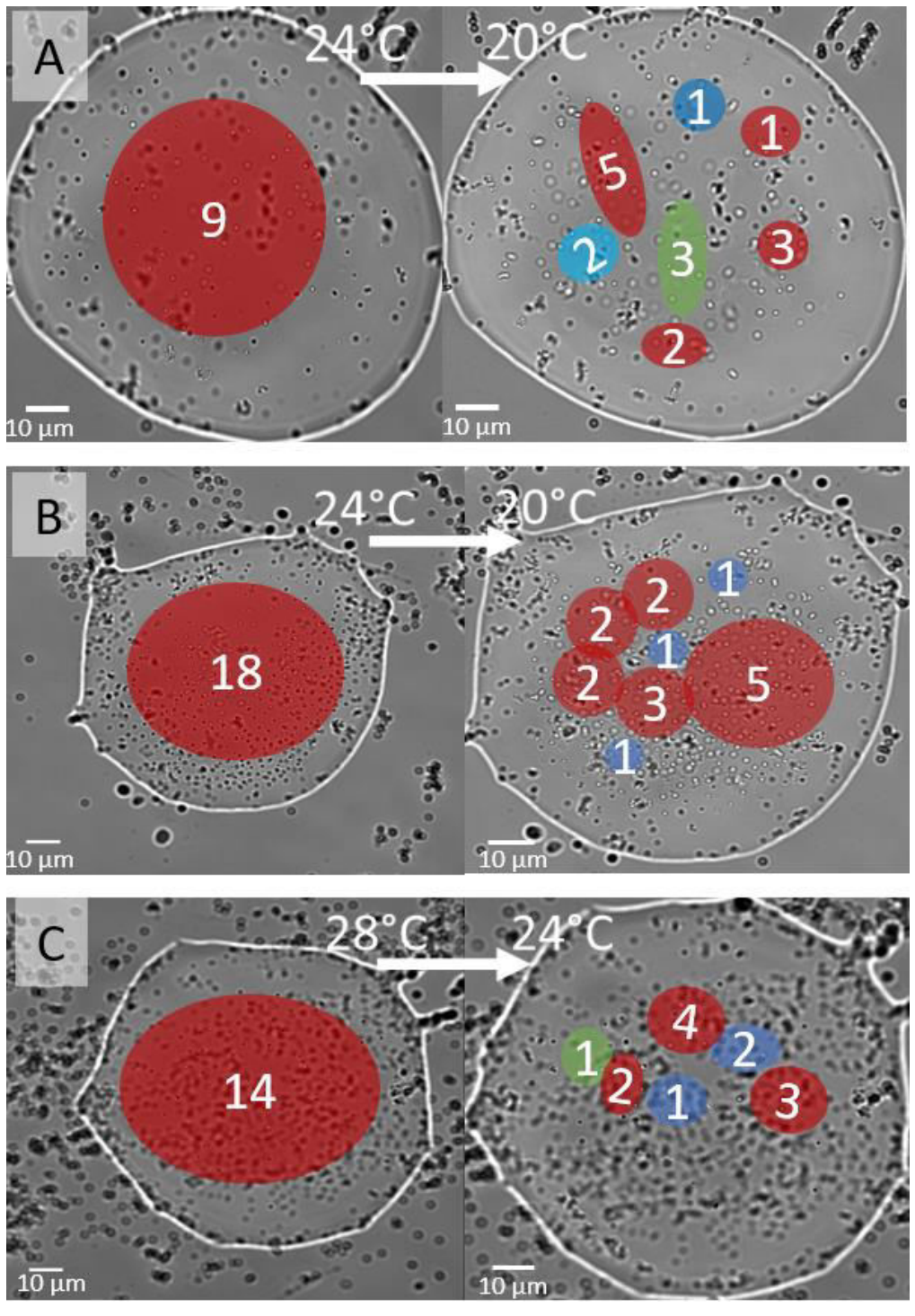

Fig. S2. Transition from homogeneous to heterogeneous phase behaviour during cooling in cuticular hydrocarbon drops with melamine beads (magnification 100x), in (A, B) *L. platythorax* and (C) *L. brunneus*. Coloured areas indicate fields with the same viscosity (red lowest and blue highest) with the number of beads measured in the field.

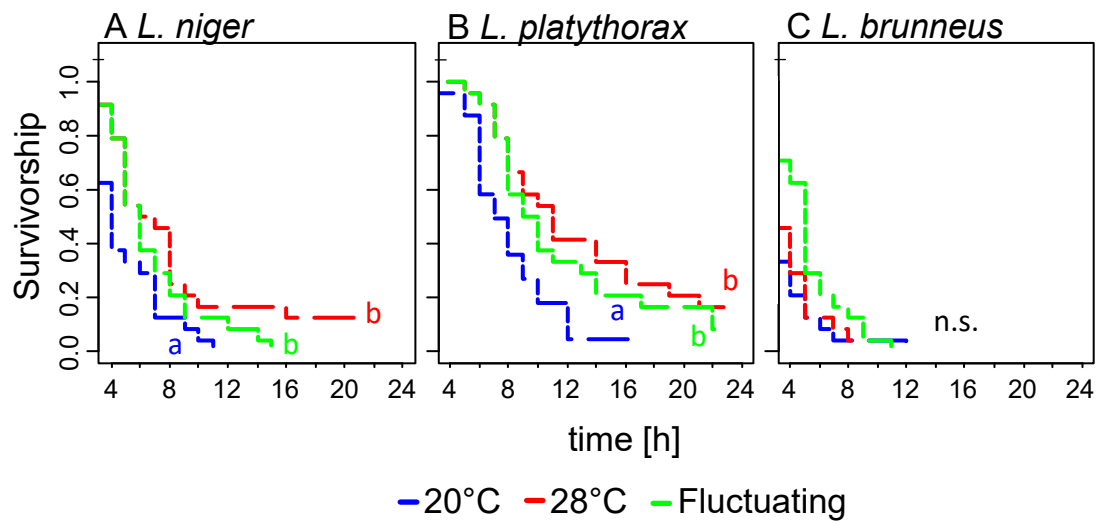

Fig. S3. Survival of (A) *Lasius niger*, (B) *L. platythorax* and (C) *L. brunneus* workers from the three acclimation treatments, only at test temperature 28 °C. Significance of differences (as indicated by letters) was calculated using separate Cox-mixed effects models for each species.

Table S1. Statistical results on the CHC analysis. The table shows results of linear mixed-effects models, with acclimation regime and fragment type (except for *L.brunneus*) as fixed factors (interactions allowed) and colony and observer (colony only for *L. brunneus*) as random effects. The dependent variables were transformed if necessary to obtain normally distributed model residuals (see table).

class	variable	Chi^2	df	p	transformation used
L. niger					
n-alkanes	acclimation	56.59	2	<0.0001	arcsin-sqrt
	fragment	0.01	1	0.91	
	acclimation x fragment	1.10	2	0.58	
monomethyl	acclimation	156.80	2	<0.0001	none
	fragment	0.04	1	0.85	
	acclimation x fragment	0.062	2	0.73	
dimethyl alkanes	acclimation	97.60	2	<0.0001	none
	fragment	0.66	1	0.42	
	acclimation x fragment	0.03	2	0.84	
trimethyl alkanes	acclimation	3.91	2	0.14	arcsin-sqrt
	fragment[2]	15.54	1	<0.0001	
	acclimation x fragment	2.06	2	0.36	
alkenes	acclimation	22.80	2	<0.0001	none
	fragment	0.65	1	0.42	
	acclimation x fragment	1.59	2	0.45	
L. platythorax					
n-alkanes	acclimation	15.60	2	0.0004	sqrt
	fragment[1]	27.56	1	<0.0001	
	acclimation x fragment	3.53	2	0.17	
monomethyl[3]	acclimation	228.06	2	<0.0001	none
	fragment	1.01	1	0.32	
	acclimation x fragment	0.06	2	0.97	
dimethyl alkanes[3]	acclimation	1.60	2	0.45	sqrt
	fragment	2.26	1	0.13	
	acclimation x fragment	0.76	2	0.68	
trimethyl alkanes	acclimation	174.71	2	<0.0001	none
	fragment[2]	37.85	1	<0.0001	
	acclimation x fragment	2.54	2	0.28	
L. brunneus					
n-alkanes	acclimation	35.41	2	<0.0001	arcsin-sqrt
monomethyl	acclimation	29.37	2	<0.0001	sqrt
dimethyl alkanes	acclimation	1.48	2	0.48	log
alkenes	acclimation	60.42	2	<0.0001	arcsin-sqrt
methyl alkenes	acclimation	65.13	2	<0.0001	arcsin-sqrt
alkadienes	acclimation	22.65	2	<0.0001	arcsin-sqrt

[1]more *n*-alkanes in small fragments; [2]less trimethyl alkanes in small fragments; [3]according to Shapiro-Wilks test, model residuals deviated from normal distribution, but histograms showed a near-normal distribution. For these two cases, we performed a permutational ANOVA (command *adonis*, package *vegan*) with the same parameters as in the linear mixed-effects models, and obtained similar results. Therefore, we report linear mixed-model results above also for these cases.

Table S2. PERMANOVA results on the effects of fluctuation per se, temperature treatment, and colony on CHC variation. To test whether fluctuating conditions differed systematically from constant ones, we created two variables, 'const/fluct' (constant vs. fluctuating conditions) and 'temperature' (nested in const/fluct, with the two factor levels 20 °C and 28°C). Interactions between colony and both factors are included in the model. The table shows df, pseudo-F, R^2 and p values.

		df	pseudo-F	R^2	p
Lasius niger	const/fluct	1	0.8	0.003	0.48
	colony	11	8.3	0.32	0.001
	temperature	1	65.6	0.23	0.001
	colony x const/fluct	11	1.0	0.039	0.42
	temperature x colony	11	1.0	0.039	0.37
Lasius platythorax	const/fluct	1	1.3	0.003	0.28
	colony	11	21.4	0.50	0.001
	temperature	1	98.9	0.21	0.001
	colony x const/fluct	11	1.3	0.031	0.16
	temperature x colony	11	1.2	0.027	0.22
Lasius brunneus	const/fluct	1	23.3	0.16	0.001
	colony	10	4.0	0.27	0.001
	temperature	1	18.6	0.13	0.001
	colony x const/fluct	8	1.6	0.086	0.068
	temperature x colony	6	2.3	0.094	0.008

Table S3. Statistical results on the survival assays. The table shows results of Cox mixed-effects models, with df, χ^2 and p values. Firstly, we constructed a comprehensive model with all test temperatures, species, and acclimation treatments. To further understand specific effects, we then created two models specific to a test temperature (20 °C and 28 °C). Then, acclimatory effects were tested in separate models for each combination of test temperature and species. Finally, to compare survival effects across species, we created acclimation treatment-specific models. Since the time of death was uncertain for some ants, we conducted two parallel analysis, treating them as if they had died a) in the first hour of the experiment or b) directly before the first observation.

			Unknown deaths treated as death in the first hour		Unknown deaths treated as death directly before observation	
Dataset	Fixed effect	Df	χ^2	p	χ^2	P
Comprehensive	Acclimation	2	28.15	<0.001	32.67	<0.001
	Species	2	39.08	<0.001	37.80	<0.001
	Test temperature	1	131.53	<0.001	170.72	<0.001
	Acclimation x species	4	16.33	0.003	17.37	0.002
	Acclimation x test temperature	2	8.49	0.014	13.16	0.001
Specific to test temperature 20 °C	Acclimation	2	5.05	0.080	4.69	0.096
	Species	2	50.07	<0.001	51.65	<0.001
	Acclmation x species	4	7.03	0.134	6.96	0.138
Specific to test temperature 28 °C	Acclimation	2	27.61	<0.001	27.44	<0.001
	Species	2	26.10	<0.001	26.57	<0.001
	Acclimation x species	4	12.50	0.014	12.84	0.002
Specific to test temperature and species						
L. niger 20 °C	Acclimation	2	1.98	0.371	1.98	0.371
L. niger 28 °C	Acclimation	2	17.00	<0.001	17.16	<0.001
L. platythorax 20°C	Acclimation	2	9.28	0.010	9.28	0.010
L. platythorax 28 °C	Acclimation	2	18.89	<0.001	18.89	<0.001
L. brunneus 20 °C	Acclimation	2	1.00	0.605	0.77	0.679
L. brunneus 28 °C	Acclimation	2	4.16	0.125	3.95	0.139
Specific to acclimation treatment						
20 °C acclimation	Test temperature	1	63.69	<0.001	97.45	<0.001
	Species	2	25.58	<0.001	27.59	<0.001
	Test temperature x species	2	1.84	0.400	0.19	0.908
28 °C acclimation	Test temperature	1	24.95	<0.001	39.72	<0.001
	Species	2	38.98	<0.001	40.50	<0.001
	Test temperature x species	2	5.31	0.070	11.02	0.004
Fluctuating acclimation	Test temperature	1	44.88	<0.001	52.82	<0.001
	Species	2	23.70	<0.001	24.03	<0.001
	Test temperature x species	2	0.65	0.72	1.02	0.599

Dataset S1. Cuticular hydrocarbon profile of *L. niger*. The table shows retention index and mean abundance (± standard error) for each hydrocarbon. See also Wittke et al. (2022).

	retention index	abundance (%)
n-C25	25.01	0.26 ± 0.05
n-C26	26	0.13 ± 0.02
n-C27	27	2.44 ± 0.34
5,11-;5,13-DiMeC27	27.81	0.14 ± 0.02
n-C28	28	0.39 ± 0.04
4-;2-MeC28	28.61	0.28 ± 0.03
C29-alkene	28.8	0.31 ± 0.06
n-C29	28.97	3.08 ± 0.31
13-;15-MeC29	29.27	1.53 ± 0.07
5-MeC29	29.49	2 ± 0.17
11,15-DiMeC29	29.56	0.4 ± 0.04
9,15-DiMeC29	29.65	3.83 ± 0.24
3-MeC29	29.73	0.56 ± 0.08
5,15-DiMeC29	29.77	2.88 ± 0.14
7,11,15-TriMeC29	29.92	1.16 ± 0.1
n-C30	29.98	0.51 ± 0.06
5,9,13-TriMeC29	30.04	0.9 ± 0.07
12-;13-;14-;15-MeC30; cf. 3,7,15-TriMeC29	30.32	1.13 ± 0.04
2-;4-MeC30	30.56	2.17 ± 0.1
C31-ene 1	30.77	1.67 ± 0.13
C31-ene 2	30.85	0.44 ± 0.03
n-C31	30.97	2.21 ± 0.15
Unknown; RI = 31.13	31.13	0.48 ± 0.1
9-;11-;13-;15-MeC31	31.32	9.95 ± 0.29
cf. 5-MeC31	31.54	1.34 ± 0.17
9,23-DiMeC31	31.69	17.59 ± 0.51
5,x-DiMeC31 (x=13;15)	31.84	6.51 ± 0.32
7,x,y-TriMeC31 (x=11,y=15?)	31.92	1.97 ± 0.13
3,9-;3,11-DiMeC31	32.02	3.46 ± 0.09
cf. 11-;12-;13-;14-;15-;16-MeC32	32.29	2.15 ± 0.07
10,14-;x.16-DiMeC32	32.58	2.46 ± 0.08
C33-alkene	32.75	0.96 ± 0.07
6,14-;6,16-DiMeC32; 3-MonoMeC32	32.85	0.37 ± 0.05
Unknown; RI = 33.04	33.04	0.52 ± 0.04
Unknown; RI = 33.17	33.17	0.27 ± 0.03
9-;11-;13-;15-MeC33	33.3	3.55 ± 0.14
11,15-DiMeC33	33.62	1.27 ± 0.15
9,x-DiMeC33 (cf. x=15)	33.7	7.36 ± 0.3
5,15-;5,17-DiMeC33	33.83	2.06 ± 0.16
7,x,y-TriMeC33	33.98	0.81 ± 0.06
3,9-;3,11-DiMeC33	34.1	1.84 ± 0.11
cf. C34 MonoMe	34.33	0.61 ± 0.05
unknown; RI = 34.61	34.61	0.75 ± 0.06
11-;13-;15-;17-MeC35	35.33	0.54 ± 0.04
cf. 11,23-DiMeC35	35.64	2.39 ± 0.12

x,y-DiMeC35	35.76	0.68 ± 0.09
Unknown; RI = 35.95	35.95	0.22 ± 0.03
Unknown; RI = 36.08	36.08	0.17 ± 0.03
Unknown; RI = 36.28	36.28	0.16 ± 0.02
Unknown; RI = 36.6	36.6	0.21 ± 0.03
Unknown; RI = 37.27	37.27	0.12 ± 0.02
cf. 11,23-DiMeC37	37.6	0.81 ± 0.09

Dataset S2. Cuticular hydrocarbon profile of *L. platythorax*. The table shows retention index and mean abundance (± standard error) for each hydrocarbon. See also Wittke et al.(2022)

	retention index	abundance (%)
n-C27	27.05	0.17 ± 0.03
n-C28	28.01	0.23 ± 0.05
n-C29	29.02	0.55 ± 0.08
n-C30	30.02	0.39 ± 0.1
n-C31	31.02	0.52 ± 0.09
7-MeC31	31.44	0.02 ± 0
13,17-DiMeC31	31.57	0.03 ± 0.01
7,x-DiMeC31	31.67	0.27 ± 0.04
5,x-DiMeC31	31.83	0.01 ± 0
n-C32	32.03	0.2 ± 0.04
5,9,15-TriMeC31	32.1	0.07 ± 0.01
cf 10-;11-;12-;13-MeC32	32.33	0.17 ± 0.02
8,x-DiMeC32	32.63	0.32 ± 0.05
6,x-DiMeC32	32.76	0.06 ± 0.01
8,12,16-TriMeC32	32.93	0.04 ± 0.01
n-C33	33.01	0.52 ± 0.05
17-;15-;13-;11-;9-;7-MonoMeC33	33.37	3.51 ± 0.18
cf 11,15-;13,17-DiMeC33	33.56	2.07 ± 0.12
9,x-;11,x-;13,x-DiMeC33	33.65	3.83 ± 0.25
7,17-;7,19-;7,21-DiMeC33	33.7	3.66 ± 0.18
5,9-;5,15-DiMeC33	33.81	3.96 ± 0.2
7,17,21-TriMeC33	33.94	4.51 ± 0.34
5,9,17-TriMeC33	34.08	3.6 ± 0.14
11-;12-;13-;14-;15-;16-;17-MeC34	34.33	1.59 ± 0.06
unknown TriMeC34	34.59	3.04 ± 0.08
8,12,16-TriMeC34	34.95	1.2 ± 0.07
4,8,x-TriMeC34	35.18	0.1 ± 0.01
13-;15-;17-MonoMeC35	35.31	5.77 ± 0.18
13,21-;11,x-DiMeC35	35.33	14.46 ± 0.71
7,19-;7,21-DiMeC35	35.71	7.29 ± 0.34
cf 11,x,23-TriMe35	35.8	4.66 ± 0.28
7,x,y-TriMeC35	35.95	5.45 ± 0.38
3,11-DiMeC35	36.09	3.45 ± 0.11
10-;11-;12-;13-;14-;15-;16-;17-;18-MeC36	36.32	1.41 ± 0.06
unknown TriMeC36	36.58	1.97 ± 0.06
8,12,22-TriMeC36	36.96	0.74 ± 0.06
13-;15-;17-MeC37	37.3	2.21 ± 0.14
9,x-;11,x-;13,x-;15,x-DiMe37	37.6	5.73 ± 0.3
7,23-;7,25-DiMeC37	37.69	2.81 ± 0.12
7,17,25-;7,19,23-;9x,y-TriMeC37)	37.98	4.93 ± 0.14
3,11-DiMeC37 and (much less) 5,9,15-TriMeC37	38.07	1.36 ± 0.08

cf. internally branched MonoMeC39	39.33	0.44 ± 0.05
7,x-;11,x-;13,x-;15,x-DiMeC39	39.58	1.55 ± 0.16
5,27-DiMeC39 (tentatively)	39.78	0.25 ± 0.04
7,x,y-TriMeC39	39.92	0.54 ± 0.05
cf 11,x-DiMeC41	NA	0.13 ± 0.02
cf 7,x-DiMeC41	NA	0.22 ± 0.05

Dataset S3. Cuticular hydrocarbon profile of *L. brunneus*. The table shows retention index and mean abundance (± standard error) for each hydrocarbon.

	retention index	abundance (%)
n -C23	22.97	0.11 ± 0.02
n -C24	23.97	0.1 ± 0.02
n -C25	24.98	0.17 ± 0.03
cf *n*- C26	25.99	0.23 ± 0.03
n -C27	27	0.74 ± 0.09
cf 4-MeC27	27.72	0.12 ± 0.03
n -C28	27.99	0.67 ± 0.07
n -C29	29	2.33 ± 0.2
11-;13-MeC29	29.31	0.04 ± 0.01
9-MeC29	29.36	0.15 ± 0.02
3-MeC29	29.75	0.65 ± 0.08
n -C30	30.01	0.97 ± 0.09
C31-ene	30.67	1.14 ± 0.06
C31-ene	30.84	0.59 ± 0.06
n -C31	31.01	3.19 ± 0.26
11-MeC31	31.34	2.71 ± 0.17
9-MeC31	31.38	0.37 ± 0.13
7-MeC31	31.43	1.8 ± 0.11
5-MeC31	31.53	0.59 ± 0.02
11,15-DiMeC31	31.59	0.57 ± 0.02
11,x-;9,x-DiMeC31 and C32-ene	31.69	1.11 ± 0.04
3-MeC31 and 5,x-DiMeC31	31.77	2.32 ± 0.13
n -C32	32.03	0.75 ± 0.05
unknown internally branched monomethyl alkane (C32)	32.33	0.12 ± 0.02
C33-diene	32.55	13.96 ± 0.43
C33-ene	32.71	11.98 ± 0.24
C33-ene	32.88	3.08 ± 0.2
n -C33	33.05	1.67 ± 0.13
unknown C33-methyl-branched alkene	33.1	0.83 ± 0.06
unknown methyl-branched alkene (C33)	33.2	0.35 ± 0.03
11-;13-;15-;17-MeC33	33.34	3.86 ± 0.17
9-MeC33	33.4	0.56 ± 0.08
7-MeC33	33.45	3.38 ± 0.14
5-MeC33	33.55	2.09 ± 0.06
unkown	33.59	0.26 ± 0.05
11,23-DiMeC33	33.69	2.58 ± 0.09
5,x-DiMeC33	33.82	1.48 ± 0.06
unknown	34.05	0.45 ± 0.04
unknown	34.35	0.21 ± 0.04
unknown	34.48	0.14 ± 0.04
C35-diene	34.58	16.24 ± 0.42
C35-ene	34.73	6.89 ± 0.19
C35-ene	34.92	0.7 ± 0.07
C35-diene	35.07	0.57 ± 0.06
C35-methyl-branched alkene	35.11	0.95 ± 0.09

unknown	35.22	0.13 ± 0.02
13-;15-;17-MeC35	35.34	1.18 ± 0.07
7-MeC35	35.48	0.43 ± 0.05
unknown unsaturated	35.65	0.48 ± 0.06
unknown unsaturated	35.72	0.29 ± 0.04
5,x-DiMeC35	35.83	0.3 ± 0.04
unknown saturated	36.07	0.1 ± 0.02
C37-diene	36.4	0.14 ± 0.04
unknown	36.46	0.15 ± 0.04
C37-diene	36.61	1.71 ± 0.13
C37-ene and C37-diene	36.73	0.69 ± 0.06
C37-ene	36.74	0.23 ± 0.07
C37-diene	36.82	0.22 ± 0.03
unknown unsaturated	37.09	0.13 ± 0.03
unknown	37.34	0.09 ± 0.02